Carbohydrate Polymers 378 (2026) 124904

Contents lists available at ScienceDirect

Carbohydrate Polymers

journal homepage: www.elsevier.com/locate/carbpol

Review

Starch aerogels as nutraceutical carriers: Experimental and computational strategies for designing a delivery system

Giulia Clare [a], Pedro N. Simões [a], Irina Smirnova [b], Luísa Durães [a,*]

[a] University of Coimbra, CERES, Department of Chemical Engineering, 3030-790, Coimbra, Portugal
[b] Institute of Thermal Separation Processes, Hamburg University of Technology, 21073, Hamburg, Germany

ARTICLE INFO

Keywords:
Aerogel
Starch
Molecular simulation
Computational modeling
Nutraceutical delivery
Carrier

ABSTRACT

The exceptional properties of aerogels explain their growing applicability in different research areas. In the case of nutraceutical delivery, they hold the potential to improve the common challenges of poor bioavailability and low stability of the bioactive ingredients, thereby enhancing intestinal delivery. Starch aerogels offer additional attractive features: biocompatibility, potential cost reduction, and abundance of raw materials. This review explores the development of starch aerogels as carriers for nutraceutical delivery, and how it can be rationalized with molecular simulation. The fundamentals of starch aerogels and the existing literature on the carriers are explored, including synthesis procedure, morphology, nutraceutical loading, and characterization of the resulting delivery system. Molecular simulation is identified as a key tool for examining properties and interactions occurring at the nano- and sub-nanoscale. The current gaps in the field are critically discussed, and trending topics for future research are identified. A computational-assisted design combined with a systematic approach to production routes is needed to further develop the field of starch aerogels for nutraceutical delivery, in addition to assessing toxicity, stability during storage, and scale-up viability.

1. Introduction

Aerogels are a class of nanostructured materials that typically exhibit a highly porous structure (total porosity usually in the range 80–99 %), with predominance of mesopores (pore diameter between 2 and 50 nm), resulting in very low bulk density (0.01–0.5 g cm^{-3}) and high specific surface area (150–1200 m^2 g^{-1}) (García-González et al., 2019; Maleki et al., 2016; Vareda et al., 2018). The microscopic features of aerogels translate into attractive bulk characteristics, such as thermal and sound insulation (Maleki et al., 2016). Aerogel properties can be tuned *via* matrix type (organic, inorganic, or composite material), synthesis route, and surface modification (*e.g.*, functionalization, coating) (Dhua et al., 2022; Zhao et al., 2018). Owing to this exceptional versatility, aerogels are used across aerospace, construction, and petrochemical fields, and, more recently, in environmental, biomedical, and pharmaceutical applications.

Despite extensive work in drug delivery, aerogels remain underused for encapsulating food and nutritional ingredients, *i.e.*, nutraceuticals (Abdullah et al., 2022; García-González et al., 2021; Gibowsky et al., 2025; Manzocco et al., 2021). The positive effect of these ingredients is often hindered by poor absorption. Aerogel-based carriers are a promising way to address this limitation and improve delivery, since their high surface area enables high loading capacity, and targeted and controlled release can be achieved by tuning the material properties (Dhua et al., 2022; García-González et al., 2021; Gonçalves et al., 2018; Manocha et al., 2022).

Traditionally, inorganic matrices – especially silica – have dominated research and industrial applications. Unlike inorganic aerogels, bioaerogels derived from natural polymers offer biodegradability, sustainable sourcing, and biocompatibility, aligning with the requirements of food-grade delivery systems (Abdullah et al., 2022; Zhao et al., 2018). Several recent reviews have surveyed food-related uses of bioaerogels, discussing their properties and production processes from a broad perspective and providing only brief overviews of the various possible precursors (Abdullah et al., 2022; Dhua et al., 2022; Manzocco et al., 2021; Selvasekaran & Chidambaram, 2022).

Starch is often identified as a promising yet underexplored polysaccharide, owing to its abundance, low cost and universal non-toxicity (Abdul Khalil et al., 2023; Zheng et al., 2020). These attributes have motivated reviews that further explore the potential of starch-based

* Corresponding author.
E-mail address: luisa@eq.uc.pt (L. Durães).

https://doi.org/10.1016/j.carbpol.2026.124904
Received 11 October 2025; Received in revised form 10 December 2025; Accepted 6 January 2026
Available online 7 January 2026

carriers. Sun et al. (2023) discussed trends and prospects for starch-based nutraceutical delivery systems, highlighting their versatility and biocompatibility, while Rostamabadi et al. (2019) focused specifically on starch-based nanodevices. However, starch aerogels are only briefly mentioned in these works and are not treated as a distinctive category of delivery systems. Conversely, notable attempts to review the production routes and property optimization of starch aerogels were made by F. Zhu (2019) and Zheng et al. (2020), but these works lack a detailed discussion on their use as carriers of bioactive ingredients.

Existing reports on starch aerogels for nutraceutical delivery focus primarily on experimental characterization of the carrier's structural and physical properties rather than delivery performance, and they overlook one essential aspect: understanding the interactions between the matrix and the nutraceutical and, in multi-nutrient systems, the interactions among co-encapsulated nutraceuticals. To date, the studies that acknowledge the importance of these interactions rely mainly on limited information obtained from experimental techniques such as Fourier transform infrared (FTIR) spectroscopy and X-ray diffraction (XRD) (Yang et al., 2024; Zhang, Li, et al., 2023).

Computational approaches can therefore provide additional insight and improve experimental efficiency in carrier design. Among them, molecular simulation is a powerful tool for representing real molecular systems and capturing their physical and chemical behavior, enabling the study of property evolution, dynamics, and interactions (Braun et al., 2019). Although still underexplored, it is essential for achieving molecular-level understanding of delivery systems.

It is clear that there is a need to systematize and rationalize the literature on starch-based aerogels for nutraceutical delivery to better understand current progress and remaining challenges. This review aims to fill this gap and to demonstrate how molecular simulation can further advance the field. We first define "nutraceutical" and outline key challenges, then discuss relevant aspects and properties of starch. We next summarize the main steps and technologies for synthesizing and producing the aerogel carrier, along with case studies from the literature. We then discuss the role of molecular simulation in the study of nutraceutical delivery systems, and conclude with key findings and future perspectives.

2. Nutraceutical delivery: Concepts and challenges

The term "*nutraceutical*" was coined by Stephen De Felice in 1989 and later clarified in a 1994 press release as "*any substance that may be considered a food or part of a food and [that] provides medical or health benefits, including the prevention and treatment of disease*". The word combines "nutrition" and "pharmaceutical" to describe what lies between the conventional concepts of foods and drugs (Wildman, 2007). The original definition is indeed broad. Despite attempts by some organizations to narrow it, the term remains contested, and several authors have proposed different meanings (Chopra et al., 2022).

Siddiqui and Moghadasian (2020) distinguish between two concepts within the broader category of dietary supplements: nutraceuticals and nutrition supplements. In their view, nutraceuticals encompass specific bioactive substances – such as plant extracts and phytochemicals – whereas nutrition supplements are intended simply to augment daily nutrient intake from food. In a similar perspective, Puri et al. (2022) describe nutraceuticals as nutrient formulations specially designed to meet dietary needs and to prevent or treat disease. They further differentiate nutraceuticals from food supplements: the former include pro- and pre-biotic foods for special medical uses, while the latter encompass minerals, vitamins and functional foods.

Both nutraceuticals and dietary supplements are non-pharmaceutical and non-medical products sold in dosage forms (*e.g.*, tablets, capsules, syrups). According to Chopra et al. (2022), the distinction between them lies in their purpose: nutraceuticals are intended for prophylactic or therapeutic use, whereas dietary supplements primarily support nutrient intake and prevent deficiencies. Conversely, other authors adopt a broader definition. Gonçalves et al. (2018) and Manocha et al. (2022) include nutrient supplements (*e.g.*, minerals and vitamins) as a subtype of nutraceuticals, following De Felice's original conceptualization.

The lack of a clear and globally accepted definition can be attributed to a heterogeneous regulation worldwide. In Europe, the legislation does not explicitly use the term nutraceuticals. The regulatory framework instead refers to food supplements – concentrated sources of nutrients or other substances with nutritional or physiological effects, marketed in dose form (*e.g.*, capsules, tablets, sachets, ampoules, drop-dispensing bottles). These include proteins, vitamins, minerals, and other substances with nutritional benefits and are regulated by the European Food Safety Authority (EFSA) (EFSA, 2022; EPCEU, 2002).

In this review, we adopt De Felice's broad classical definition of nutraceutical because of its generality. Accordingly, nutraceuticals encompass a wide range of substances whose different structures and properties lead to varied physiological effects in the body. They are absorbed in the intestine, and a common challenge is their poor bioavailability, often associated with reduced stability and low solubility in intestinal fluids (Manocha et al., 2022).

During processing and storage, exposure to light, oxygen, humidity, and temperature can degrade many nutraceuticals because of their limited chemical and physical stability. After ingestion, variable pH and enzymatic activity along the gastrointestinal tract further compromise integrity. For example, light and oxygen can damage phenolic compounds (Araujo et al., 2024). Without adequate protection, nutraceuticals may reach the intestine chemically altered and partially or fully lose bioactivity. Solubility is another recurring issue: compounds must be dissolved in the intestinal fluid to be absorbed. Many nutraceuticals – such as β-carotene (Zhang, Wang, et al., 2023) and curcumin (Alavi & Ciftci, 2024a) – are poorly water-soluble, leading to low bioavailability. Consequently, conventional supplements often resort to high doses to overcome stability and solubility limitations (Gonçalves et al., 2018; Manocha et al., 2022).

In a nutshell, effective carrier systems for nutraceutical delivery should: (i) protect the nutrient during shelf-life and passage through the gastrointestinal tract (from pH changes and enzymes); (ii) preserve chemical integrity and bioactivity so benefits are retained after absorption; (iii) provide sufficient loading capacity to achieve the intended dose; (iv) enable intestinal targeting and, when needed, controlled release; (v) enhance solubility/dissolution in intestinal fluid (*via* suitable chemical or physical functionalities); (vi) be food-grade and safe; (vii) feature sensory properties when relevant (Gonçalves et al., 2018).

3. Starch structure and transformation

Starch is a polysaccharide composed of two macromolecules – amylose and amylopectin (Fig. 1). Both are glucose-based and their ratio depends on the starch source, *e.g.*, maize, potato, wheat, rice. Typically, starch contains ~70–80 % amylopectin and ~20–30 % amylose, though high-amylose and waxy (amylopectin-rich) starches are also commercially available (S. Wang et al., 2015; Zheng et al., 2020). Amylose is a relatively small, essentially linear polymer of (1 → 4)-linked α-D-glucopyranosyl units. Amylopectin is larger and highly branched: most linkages are (1 → 4), with branches introduced by (1 → 6) bonds. Branch points occur roughly every 20–30 units (Goodfellow & Wilson, 1990; Karim et al., 2000).

Native starch is organized in semi-crystalline granules (Fig. 2) with ~30–45 % crystallinity (S. Wang et al., 2015; Eliasson, 2010). The granules feature an amorphous bulk core, composed of disordered amylose and amylopectin chains. Concentric growth rings surround the core: amylopectin outer branches form double helices, organized in crystalline domains, while the intervening amorphous regions are rich in amylose (S. Wang et al., 2015).

Under appropriate conditions, starch undergoes two key processes: gelatinization and retrogradation. These transformations are important

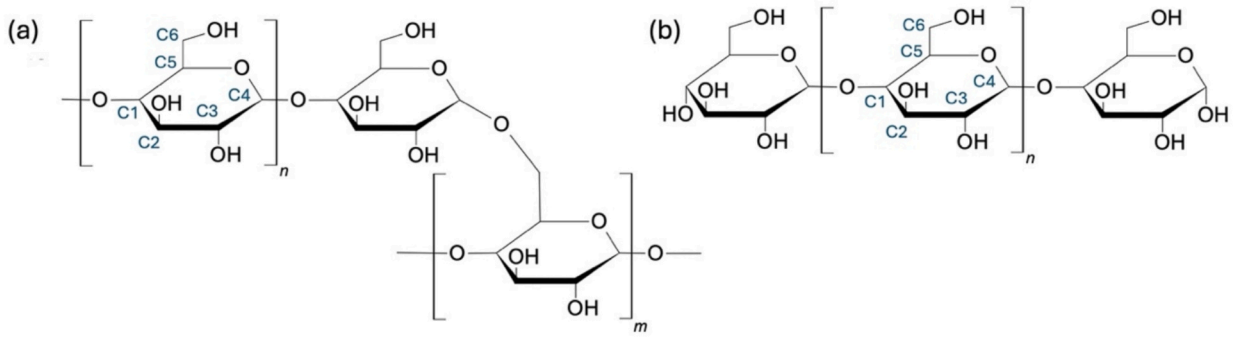

Fig. 1. (a) Amylopectin and (b) amylose macromolecular structures.

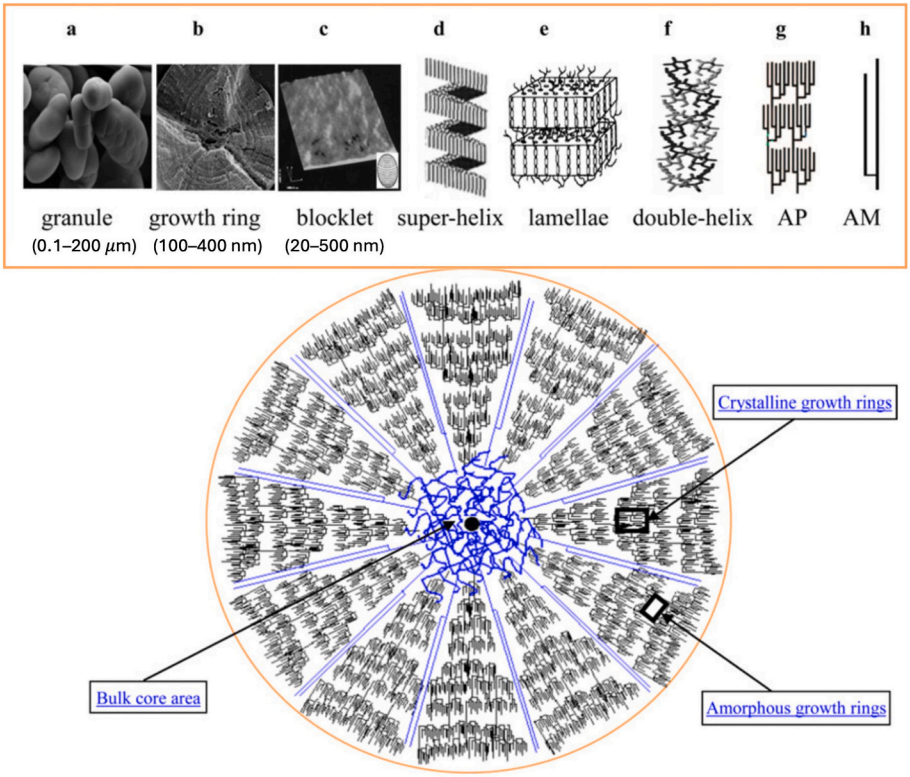

Fig. 2. Hierarchical structure of starch, from Scanning Electron Microscopy (SEM) images of (a) granules and (b) growth rings, to (c) blocklets by Atomic Force Microscopy, and (d–h) representations of super helix, lamellar, and double-helical structures, plus amylopectin (AP) and amylose (AM). Schematic distribution of AP (black) and AM (blue) shown below (not to scale). Reproduced and adapted from S. Wang et al. (2015) with permission from John Wiley and Sons.

in food processing: gelatinization is typically induced to modify properties such as water-holding capacity, rheology, and sensory attributes, whereas retrogradation is usually undesired because it can diminish product quality, with some exceptions. Both can also occur following purchase by the consumer – for example, when cooked starch is refrigerated (Eliasson, 2010).

In the case of gelatinization, heating starch–water mixtures to ~60–130 °C (range depends on source and water content) triggers a non-equilibrium process in which water penetrates granules, and heat and hydration cause swelling and granule collapse (Hoover, 1995; S. Wang et al., 2015; Eliasson, 2010; Zheng et al., 2020). At the molecular level, double helices melt/unwind, amylose adopts random-coil conformations, and overall crystallinity decreases, followed by leaching from amorphous regions (amylopectin may also leach, though less commonly). At the macroscopic level, viscosity increases, and a paste/gel is formed, consisting of swollen, fragmented granules and leached polymers. Complete dissolution generally requires more severe conditions, such as higher temperature/pressure (Eliasson, 2010).

Upon cooling gelatinized starch and storing it at low temperature for some days, the amorphous state transits to a new, partially crystalline structure, in a process named “retrogradation” by Katz (1934). Goodfellow and Wilson (1990) proposed distinct pathways for amylose and amylopectin retrogradation (Fig. 3). For amylose, cooling promotes rapid, short-range intermolecular ordering into double helices, sometimes preceded or accompanied by phase separation. It is followed by slower aggregation into long-range ordered domains that confer crystallinity. For amylopectin, side chains first undergo a rapid random coil to double helices intramolecular transition, because helices are tethered to the main chain. Then, a slower aggregation step generates crystalline regions. While the initial intramolecular step does not directly form the 3D network, subsequent ordering of helical side chains produces rigid crystalline sections that strengthen the gel (Goodfellow & Wilson, 1990).

Moreover, these sequential phenomena enable the transformation of

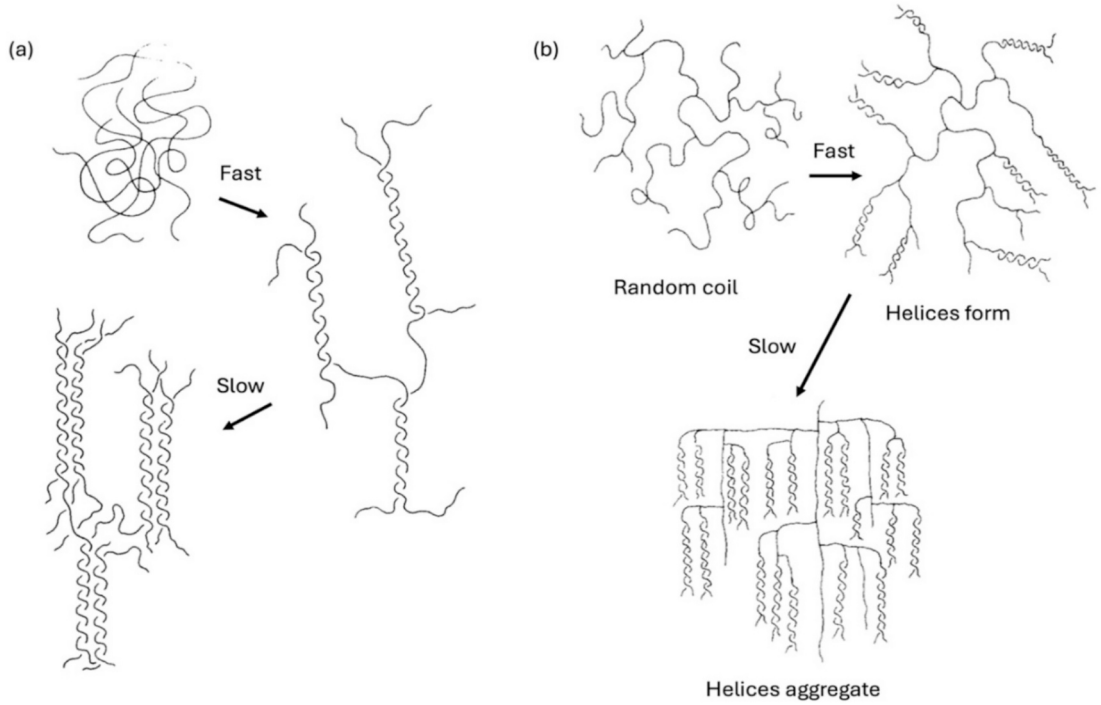

Fig. 3. Schematic representation of (a) amylose and (b) amylopectin crystallization process during retrogradation. Reproduced from Goodfellow and Wilson (1990) with permission from John Wiley and Sons.

native starch granules (see Fig. 2) into the interconnected porous network characteristic of starch gels. Consequently, the amylose-to-amylopectin ratio of the native starch is a key determinant of the properties of the resulting aerogel, as it intrinsically influences both gelatinization and retrogradation, which in turn affect the final material. These relationships are further explored in the following sections.

4. Starch-based aerogel carriers

The role of starch aerogels in nutraceutical delivery remains underexplored, despite growing interest reflected by an increasing number of studies in recent years. Table 1 compiles the current research on carrier systems based on starch aerogels for nutraceutical delivery; the selected papers are discussed in the subsections below.

It is important to note that the table includes studies in which the authors labeled the starch-based matrix as an "aerogel". Aerogels were first reported by Kistler (1931), who defined them as "*gels in which the liquid has been replaced by air, with very moderate shrinkage of the solid network*". Kistler used supercritical drying for this purpose. Today, aerogels can be produced by multiple drying methods and span a broad porosity range, and the definition of "aerogel" is still a topic under discussion. Although some reports in Table 1 describe materials with relatively low specific surface area – raising questions about whether they meet the aerogel criteria – all systems synthesized, characterized, or labeled as aerogels were included, to provide a comprehensive overview. Detailed discussions on aerogel terminology and definitions can be found in Vareda et al. (2018) and Steiner and Pierre (2023).

4.1. Synthesis and drying of starch aerogels

Fig. 4 illustrates the synthesis pathway for starch aerogels. The procedure starts with dispersing starch in water at elevated temperatures, typically 60–130 °C, triggering gelatinization. When the resulting paste is cooled and stored at low temperature (commonly 4 °C), retrogradation occurs. During this stage, physical cross-linking is triggered by the temperature drop, and the network strength increases with aging time (Zhao et al., 2018; Zheng et al., 2020).

The final step, drying, involves replacing the liquid within the gel pores with a gas, converting the gel into an aerogel. This stage is crucial, as it determines whether the material's porous structure is preserved. The three main drying methods are ambient pressure (or evaporative) drying, freeze-drying, and supercritical drying. Depending on the chosen method, a preliminary solvent exchange step may be necessary (Abdullah et al., 2022; Zhao et al., 2018).

Ambient pressure drying is the simplest method, often carried out at room temperature or under heating to evaporate the solvent. A solvent exchange – typically from water to ethanol – is sometimes used beforehand to increase volatility. However, unless surface modification is carried out to render the gel hydrophobic, intense capillary stress during evaporation leads to pore collapse and the formation of a xerogel. This results in a heavy shrinkage and significant loss of porosity at the macroscale (Dhua et al., 2022). In thermodynamic terms, this process involves crossing the liquid-gas equilibrium line, as illustrated for ethanol in case (i) of Fig. 5a (Subrahmanyam et al., 2023).

Alternative drying methods aim to prevent the formation of a liquid-gas interface, thereby reducing capillary stress and helping preserve the material's porous architecture. As illustrated in case (ii) of Fig. 5b, freeze-drying achieves this by bypassing the triple point of the solvent. In this process, the gel is first frozen, and the system pressure is then reduced to a moderate vacuum level (typically between 0.01 mbar and 0.1 mbar), allowing the frozen solvent – usually water – to sublimate (Griffin et al., 2023). When organic solvents are used, the operating temperature must be adjusted according to their sublimation conditions. Although freeze-drying is operationally simple, it is also time- and energy-intensive. Moreover, the formation of ice crystals during freezing often leads to pore enlargement and can significantly damage the mesoporous network, compromising the structural integrity of the resulting material (Abdullah et al., 2022; Zhao et al., 2018).

Supercritical drying is widely regarded as the most effective technique for producing aerogels. Since fluids in the supercritical state do not originate capillary forces, the material's porous structure is almost entirely preserved. In general, two approaches are possible: high-

Table 1
Main publications of starch-based aerogel systems[1] for nutraceutical delivery.

Carrier morphology	Starch type	Bioactive compound	Loading method	Drying method	S_{BET} / (m^2 g^{-1})	ρ_b / (g cm^{-3})	Loading capacity / (% w/w)	Reference
Thin disk	Corn, tapioca	Thymol	$scCO_2$ impregnation	$scCO_2$ drying and air drying	0.019; 0.035	NA	0.58–3.31	Milovanovic et al. (2015)
Powder	Wheat	Phytosterols	$scCO_2$ impregnation	$scCO_2$ drying	59.7 ± 0.9	0.12 ± 0.00	5.5 ± 0.1[2]	Ubeyitogullari and Ciftci (2016)
Unspecified	Maize	Vitamins E and K3	$scCO_2$ impregnation	$scCO_2$ drying	90[3]; 86[4]	NA	19.99; 8.76	De Marco and Reverchon (2017)
Unspecified	Corn	Vitamin E	$scCO_2$ impregnation	$scCO_2$ drying	NA	NA	NA	De Marco et al. (2019)
Powder (60–70 μm)	Wheat, corn	Phytosterols	$scCO_2$ impregnation	$scCO_2$ drying	62; 221	0.11 ± 0.01; 0.16 ± 0.01	10.0–19.5[2]	Ubeyitogullari et al. (2019)
Monolith	Potato	Green coffee oil	$scCO_2$ impregnation	$scCO_2$ drying	39; 185	NA	NA	Villegas et al. (2019)
Powder (100 nm)	Corn, potato, tapioca	Genistein	Soaking in ethanol solution + solvent evaporation	Freeze-drying, microwave drying, rotary vacuum drying	50–150	NA	4.24–49.01	Soleimanpour et al. (2020)
Particle (10–100 μm)	Corn	β-carotene	$scCO_2$ impregnation	$scCO_2$ drying	64.3[3]; 53.5[4]	NA	0.001–0.096[2]	Dias et al. (2022)
Monolith	Corn	Hemp seed oil and flour extracts, (*e.g.*, linoleic acid)	$scCO_2$ impregnation	$scCO_2$ drying	71.1–208.6	0.445–0.773	up to 33[2]	Lukic et al. (2022)
Particle	Corn	Polyphenols	$scCO_2$ impregnation	$scCO_2$ drying	63.6[3]; 51.7[4]	NA	NA	Araujo et al. (2023)
Monolith	Corn, potato	Quercetin	$scCO_2$ impregnation	$scCO_2$ drying	23–89	0.37–0.46	0.05–0.24[5]	Mottola et al. (2023)
Not specified	SHMP-modified corn	β-carotene	Encapsulation by dispersion in precursor solution (before gelatin.)	Freeze-drying	NA	NA	NA	Zhang, Wang, et al. (2023)
Powder	Corn + chitosan (0 %, 5 %, 75 %)	Curcumin	Soaking in ethanol solution	$scCO_2$ drying	205.9 ± 3.9[4]; 184.1 ± 2.1[4]; 187.9 ± 3.7[4]	0.151 ± 0.010[4]; 0.125 ± 0.008[4]; 0.132 ± 0.008[4]	2.41[2]; 2.75[2]; 2.44[2]	Alavi and Ciftci (2024a)
Powder	Corn with varying amylose content	Curcumin	Soaking in ethanol solution	$scCO_2$ drying	66.3 ± 1.8[4]; 170.5 ± 5.0[4]; 196.8 ± 4.2[4]	0.234± 0.01[4]; 0.158 ± 0.007[4]; 0.147 ± 0.008[4]	1.64[2]; 2.14[2]; 2.49[2]	Alavi and Ciftci (2024b)
Particle	Corn	Polyphenols from passion fruit bagasse (including piceatannol)	$scCO_2$ impregnation	$scCO_2$ drying	44.7 ± 0.3[3]; 41.1 ± 0.4[4]	NA	NA	Araujo et al. (2024)
Pieces of monolith; powder	Maize	Iron and folic acid (individual and co-delivery)	Encapsulation by dispersion in precursor solution (after gelatin.)	Freeze-drying	0.80 ± 0.04	0.140 ± 0.002	Iron: 11.05 ± 0.01; 11.03 ± 0.01; Folic acid: 0.390 ± 0.003; 0.224± 0.001	Clare et al. (2024)
Monolith	SHMP-modified corn, wheat, rice	Cannabidiol	Encapsulation by dispersion in precursor solution (before gelatin.)	Freeze-drying	Wheat starch: 2.4[3]; 1.6[4]	NA	NA	H. Li, Lv, et al. (2024)
Monolith	Potato with cellulose nanocrystals and bacterial nanocellulose	Xanthohumol and usnic acid (co-delivery)	XH: soaking in ethanol solution; UA: $scCO_2$ impregnation	$scCO_2$ drying	Starch: 183 ± 4[3]; 120± 3[4]; Starch-cellulose: 190–220[3]; 110–139[4]	NA	XH: 0.0129[2], 0.0140–0.0166[2]; UA: 0.7	Pantić et al. (2024)
Monolith	SHMP-modified wheat	Procyanidin	Encapsulation by dispersion in precursor solution (before gelatin.)	Freeze-drying	2.4[3]; 8.1 [4]	NA	1.16 ± 0.03	Yang et al. (2024)

$scCO_2$ – supercritical CO_2. NA – data not available. SHMP – sodium hexametaphosphate. XH – xanthohumol. UA – usnic acid.
[1] Materials with low surface area, but classified as aerogels by the authors, were also included.
[2] Values originally expressed in another unit by authors.
[3] Without nutraceutical.
[4] With nutraceutical.
[5] % w/w as nutraceutical/polymer, instead of % w/w nutraceutical/aerogel.

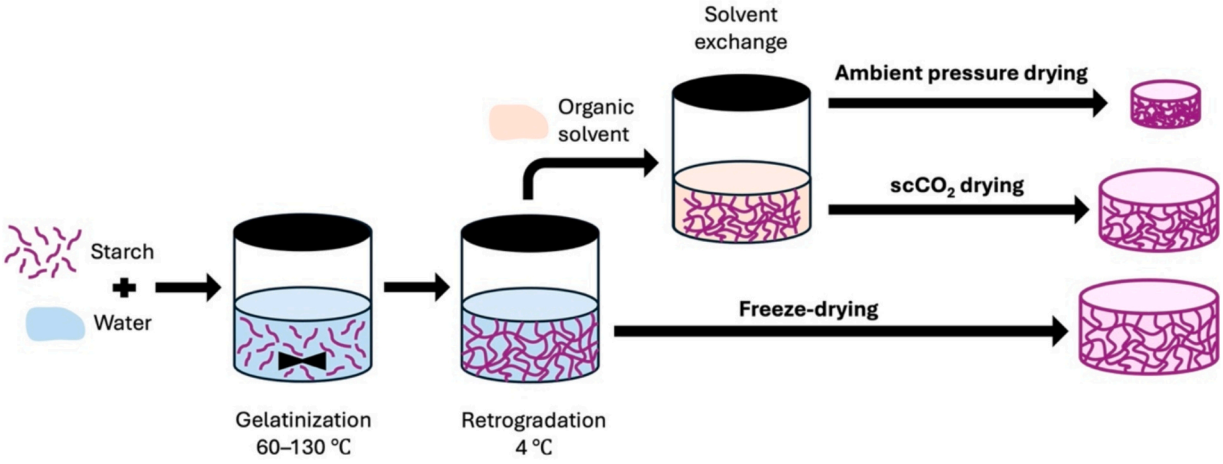

Fig. 4. Schematic of the main steps involved in the synthesis of starch aerogels: gelatinization, retrogradation, solvent exchange and drying.

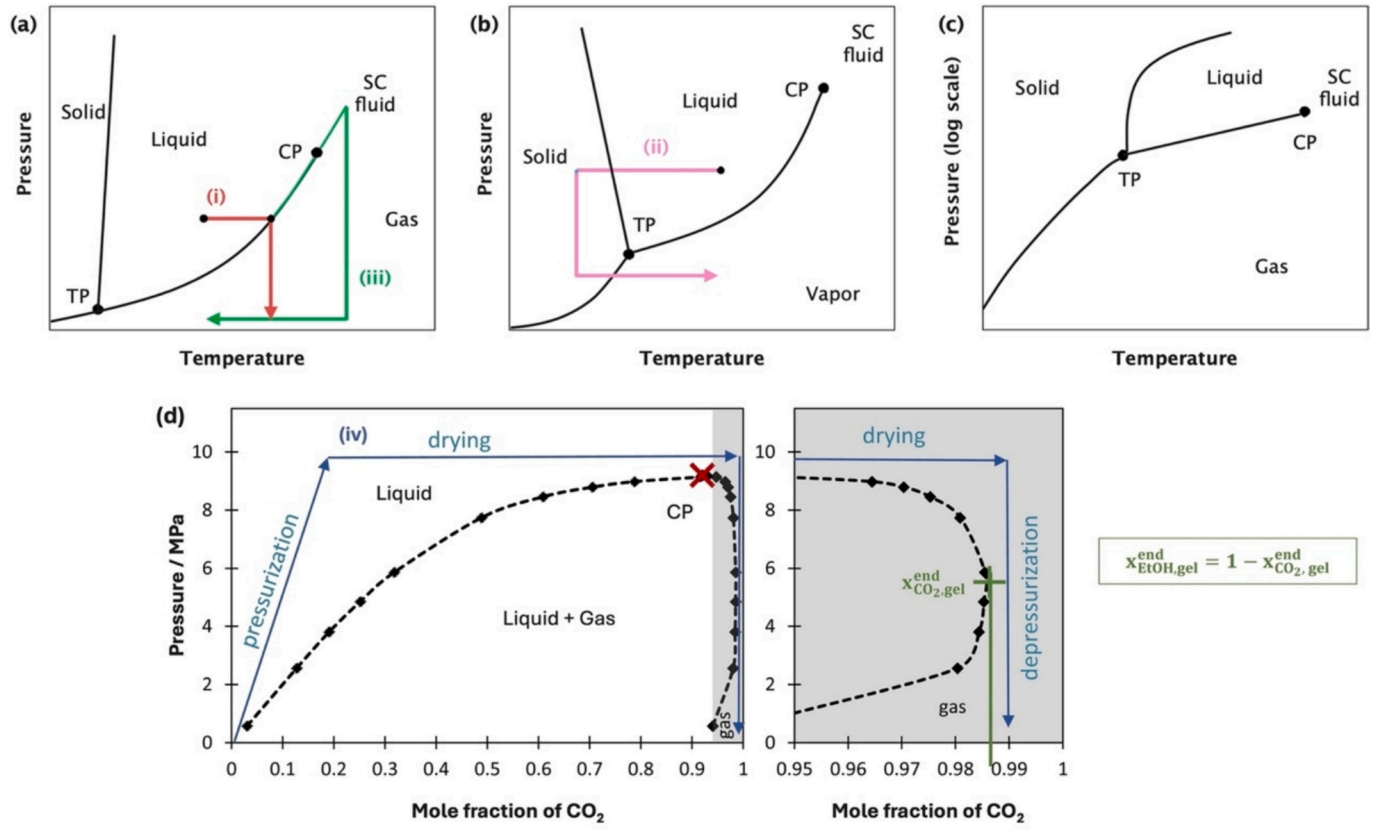

Fig. 5. Schematic P-T (pressure-temperature) diagrams of (a) ethanol, (b) water, and (c) carbon dioxide, and (d) P-x (pressure-composition) diagram of the mixture ethanol–CO_2 at 323 K (dashed line with mixture; CP marked with a red X; grey area zoomed on the right). The diagrams include schematic representations of (i) ambient pressure drying (with heating), (ii) freeze-drying, (iii) high temperature supercritical drying and (iv) supercritical drying with CO_2 operating trajectories (Griffin et al., 2023; Selmer et al., 2018; Span & Wagner, 1996; Subrahmanyam et al., 2023; Witkowski et al., 2014). Diagrams not to scale. SC – supercritical; TP – triple point; CP – critical point. Diagram (d) reproduced and adapted from Selmer et al. (2018) with permission from Elsevier.

temperature supercritical drying and supercritical drying with CO_2. In the former, the gel is heated and pressurized until the solvent – usually ethanol – reaches the supercritical state. The resulting supercritical fluid is then removed at a constant temperature, as shown in case (iii) of Fig. 5a. While this approach is effective for inorganic aerogels like silica, the harsh thermal conditions (>250 °C) can degrade organic matrices, limiting its suitability for bioaerogels.

Alternatively, supercritical drying with CO_2 offers a more compatible option for biopolymer-based systems. In this process, supercritical CO_2 ($scCO_2$) extracts the solvent from the gel, which requires the solvent – typically ethanol – to be soluble in $scCO_2$. The presence of the organic solvent in the system does not allow the operation to be represented in a single-phase P-T (pressure-temperature) diagram (see Fig. 5c). Representing the operation line in a binary phase diagram (P-x, *i.e.*, pressure-composition) requires fixing an operating temperature and identifying the corresponding critical pressure of the mixture in order to draw the

line above the critical pressure, as can be seen in case (iv) of Fig. 5d, for the ethanol–CO_2 mixture. Consequently, the operating line includes the removal of the solvent (Selmer et al., 2018; Subrahmanyam et al., 2023). Because CO_2 reaches its supercritical state at moderate temperature (critical point of CO_2: 31.05 °C, 7.38 MPa; NIST WebBook, 2025), this method is well-suited for bioaerogels and can be applied either continuously or in batch mode for organic solvent removal (Abdullah et al., 2022; Vareda et al., 2018).

Despite its advantages, supercritical drying presents some limitations. Before drying, an additional step is required to exchange water for a solvent soluble in $scCO_2$. In the case of starch aerogels, solvent exchange may cause shrinkage of the network. However, this issue can be diminished with a multi-stage solvent exchange protocol (Abdullah et al., 2022).

Regarding the drying step, CO_2 is generally recognized as safe (GRAS) by the U.S. Food and Drug Administration (FDA) for the processing of food products (US FDA, 2024). One potential limitation involves the residual presence of the organic solvent, which may remain adsorbed on the large surface area of starch aerogels. In the case of ethanol, this could pose challenges for specific consumer groups, including children or individuals sensitive to alcohol (Manzocco et al., 2021).

4.1.1. Tuning of aerogel properties

As with other types of aerogels, the synthesis conditions of starch aerogels can be adjusted to tailor their properties for specific applications. Key variables include the amylose-to-amylopectin ratio (which depends on the starch source), the initial starch concentration in water, temperature and duration of both gelatinization and retrogradation steps, and parameters specific to the drying method. These conditions directly affect essential properties of the resulting aerogel, including specific surface area, bulk density, and porosity (Zheng et al., 2020).

In general, increasing the amylose content and retrogradation time tends to produce gels with a more developed network structure with entangled amylose chains. Although these gels are often described as "stronger" (Soleimanpour et al., 2020; Zou & Budtova, 2021), authors rarely specify which mechanical properties – such as elastic modulus, compressive strength, or toughness – are being referred to. The common observation is that they are less prone to shrinkage during solvent exchange, and the resulting aerogels typically exhibit lower bulk density and higher specific surface area. Excessive amylose, however, can have the opposite effect. Druel et al. (2017) reported that pure amylose starch led to heterogeneous samples that collapsed under supercritical drying and did not produce monolithic aerogels, despite the long retrogradation times tested (up to 240 h).

Regarding crystallinity, Zou and Budtova (2021) observed that a higher amylose content promotes higher relative crystallinity, as amylose molecules tend to crystallize faster than amylopectin during retrogradation. Conversely, Soleimanpour et al. (2020) reported that a higher proportion of amylopectin can lead to the formation of well-ordered crystalline complexes within the gel network, contributing to improved mechanical stability.

The drying method plays a critical role in determining the final pore structure, particularly with respect to specific surface area. Baudron et al. (2019) compared aerogels from amylomaize starch (amylose content: 67 %) obtained *via* freeze-drying (solvent: water; freezing temperature: − 20 °C in a freezer, or − 196 °C with liquid nitrogen; drying: at 2.38 mbar for 48 h, or at 0.045 mbar for 96 h) and supercritical drying with CO_2 (solvent: ethanol; drying with 20 g/min continuous flow of CO_2 at 120 bar and 60 °C, for 3 h). The latter produced a far more favorable pore structure, with a maximum specific surface area of 197 $m^2\ g^{-1}$, whereas the freeze-dried samples exhibited large macropores caused by ice crystal formation and much lower specific surface areas (up to 7.7 $m^2\ g^{-1}$ for freezing at − 20 °C and drying at 0.045 mbar for 96 h). Similarly, H. Li, Lv, et al. (2024) reported that wheat starch aerogels prepared by freeze-drying (freezing at − 48 °C) displayed a layered porous structure, with surface area of only 2.4 $m^2\ g^{-1}$ and pore sizes ranging from 10 to 20 μm.

Moreover, the final aerogel properties can be tuned by adjusting the drying parameters, including solvent selection. Lukic et al. (2022) used acetone instead of ethanol during solvent exchange because of its higher miscibility with $scCO_2$. The authors then evaluated the effect temperature and pressure of the supercritical drying on the structural properties of the resulting aerogels. The aerogel with highest porosity (81.1 %) also presented the highest specific surface area, 208.6 $m^2\ g^{-1}$, and was dried at 45 °C and 10 MPa.

While alternative drying methods, such as microwave drying and rotary vacuum drying, have yielded promising results (Soleimanpour et al., 2020), supercritical drying with CO_2 remains the most established and effective technique for starch aerogel production.

The comparison among the studies summarized in Table 1 further confirms that supercritical drying with CO_2 is the most effective in preserving porosity, consistently yielding surface areas above 195 $m^2\ g^{-1}$ (Alavi & Ciftci, 2024a; Alavi & Ciftci, 2024b; Lukic et al., 2022; Ubeyitogullari et al., 2019). In addition to the drying method, these studies share other synthesis choices, including the use of high-amylose starch (70 % or higher), high starch concentration in water (10 %), high gelatinization temperature (95–120 °C), and intermediate retrogradation times (24–48 h). It is also important to note that incomplete gelatinization can diminish surface area due to the presence of undissolved native starch granules within the network.

On the other hand, Pantić et al. (2024) also reported surface areas as high as 220 $m^2\ g^{-1}$ for aerogels produced from potato starch (23 % amylose content), at a starch concentration of 5 %. In this case, the high surface area was achieved by the addition of cellulose nanocrystals and bacterial nanocellulose.

Additionally, several studies have explored the synthesis parameters using a generalist approach, without targeting a particular application for the final material. Notably, Zheng et al. (2020) provided a detailed analysis of the most influential synthesis factors and their impact on the physical properties of starch aerogels. Table 2 summarizes the main findings and recurring trends reported in the literature under this topic. It is important to note that this section offers only a brief overview of the conditions leading to aerogels suitable for use as nutraceutical carriers. For a more comprehensive discussion on synthesis optimization, readers are referred to the works of F. Zhu (2019) and Zheng et al. (2020).

4.2. Carrier morphology: Particle production methods

The morphology of aerogel carriers is a key factor influencing their performance in nutraceutical delivery. Polysaccharide aerogels can be produced in various shapes and sizes, including monoliths, films, and spherical particles (Zheng et al., 2020). However, in the case of starch-based aerogels, the carrier's morphology is often overlooked, limiting comparisons across studies. As summarized in Table 1, the most common forms include cylindrical monoliths, milled powders, and particles. While monoliths (typically millimeter to centimeter scale) are useful for characterizations such as mechanical testing and density measurements, they are unsuitable for oral delivery applications, and their use in simulated digestion tests may distort release profiles.

Microspheres are particularly attractive due to their flowability, ease of handling, uniformity, and lack of sharp edges (García-González et al., 2015). Several production methods exist for aerogel particles, differing in terms of shape and size. Ganesan et al. (2018), in a comprehensive review, outlined a general process flow: droplet formation, gelation (*i.e.*, gel formation), particle recovery, solvent exchange (if required), and drying. The different techniques are broadly classified according to whether droplets are formed in a gaseous or liquid medium (Fig. 6).

In case (i), the droplet is formed in a gaseous phase and then falls into a gelation or coagulation bath, where gelation occurs due to a gelling agent or condition (Ganesan et al., 2018; García-González et al., 2021). This category includes two approaches: the conventional dropping

Table 2
Influence of synthesis parameters on the properties of the resulting material[1].

Parameter	Trends for resulting properties	Key points and observations
Amylose/ amylopectin ratio	• ↑ amylose →↑ SSA, ↑ resistance to shrinkage • ↑ amylopectin → ↑ crystallinity, ↓ porosity	• High amylose content (*e.g.,* 60–80 %) favors stronger, more ramified networks resistant to shrinkage, and mesoporosity • Pure amylose starch results in a cracked network that collapses during drying • High amylopectin content (*e.g.,* >80 %) leads to incomplete dissolution, higher crystallinity and reduced porosity
Starch concentration in water	• ↑ concentration (up to a certain concentration) →↑ density, ↑ stiffness, ↓ porosity • High concentrations (>14 % *w/w*): ↓ SSA, larger pores, difficulty to handle • Low concentrations (<5 % w/w): gel is not formed	• Increasing starch concentration in a certain range (5–14 % w/w) leads to more structural integrity and stronger gels, that resist shrinkage • However, above the upper limit (>14 % w/w), the starch dispersion becomes very viscous, gel handling is constrained, and SSA decreases due to incomplete dissolution of starch granules
Gelatinization temperature	• ↑ temperature (up to a certain temperature) → ↑ SSA, ↓ density • Higher temperatures (*e.g.*> 130 °C): opposite effect	• Optimal temperature depends on type of starch (*i.e.*, amylose/amylopectin ratio) • Incomplete gelatinization can compromise surface area due to the presence of non-dissolved granules • Higher temperatures lead to a higher gelatinization degree and dissolution of starch granules, up to a limit (*e.g.*, <130 °C, depends on the type of starch) • The effect of time is rarely studied
Retrogradation conditions	• ↑ time → stronger gels, ↑ SSA, ↑ crystallinity, ↓ density	• Longer retrogradation (*e.g.*, >48 h) leads to gels with thicker and stronger pore walls, more resistant to shrinkage, and more developed and ramified network • Amylose retrogrades faster than amylopectin • Temperature is usually the same (4 °C)
Drying method	• $scCO_2$ drying →↑ SSA, mesopores prevail • Freeze-drying → prevalence of macropores, ↓ density, ↑ porosity	• $scCO_2$ and freeze-drying are the most common techniques • Shrinkage observed during solvent exchange before $scCO_2$ drying • Porous structure is well preserved with $scCO_2$ drying • Formation of ice crystals during freezing damages the porous structure

SSA – specific surface area. $scCO_2$ – supercritical CO_2.
[1] Information compiled from the references: Ubeyitogullari and Ciftci (2016); Druel et al. (2017); Baudron et al. (2019); Soleimanpour et al. (2020); Zheng et al. (2020); Mottola et al. (2023); Zou and Budtova (2023); Alavi and Ciftci (2024b).

method and spraying/atomization. In the simplest form of the dropping method, a pipette or syringe releases droplets that fall by gravity. Production capacity and particle size can be further controlled with external devices that regulate droplet formation. In such cases, droplet breakup is induced by a vibrating nozzle, electrostatic forces, or mechanical cutting. Jet cutting is a widely used technique in which a continuous liquid jet is mechanically cut. Bead size can be adjusted by varying the cutting frequency, jet speed, and nozzle diameter, enabling high production rates. By contrast, spraying/atomization involves more complex equipment that completely disintegrates the liquid jet into droplets in a gas phase or vacuum (Ganesan et al., 2018). So far, this method has not been applied to produce starch aerogel particles for nutraceutical delivery.

Case (ii) corresponds to the emulsion–gelation method, which involves two steps: emulsification and gelation. Two immiscible liquids are mixed under agitation, with an emulsifier stabilizing the emulsion. The polysaccharide solution is usually the aqueous phase, resulting in a water-in-oil (w/o) emulsion. This stable emulsion is then exposed to a chemical or physical stimulus that induces gelation and further stabilizes the droplets. The trigger depends on the polysaccharide used; in the case of starch, it is cooling. Parameters influencing this method include the w/o ratio, viscosity, surfactant concentration, and agitation rate, among others (Ganesan et al., 2018).

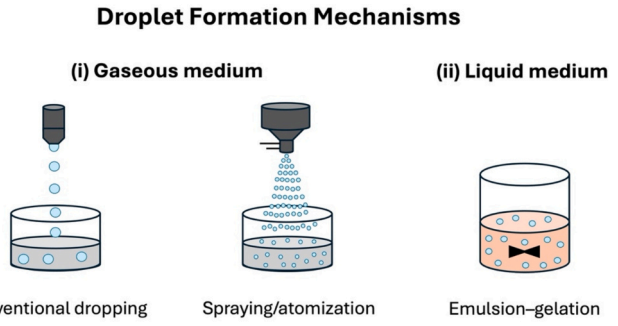

Fig. 6. Schematics of techniques for producing polysaccharide aerogel particles, grouped by the medium in which droplet formation occurs: (i) gaseous or (ii) liquid.

After particles formation by case (i) or (ii), they must be separated from the liquid medium, typically by centrifugation or filtration. Washing, usually with water, is recommended to remove the emulsion solvents and additives, *e.g.*, the surfactant. The subsequent steps follow those described in Section 4.1: solvent exchange, if required, and drying. In terms of particle size, emulsion–gelation produces microspheres of 10–500 μm, whereas jet cutting yields larger beads ranging from 200 μm to 10 mm (Ganesan et al., 2018).

Dias et al. (2022) produced corn starch aerogel particles using the emulsion–gelation method, followed by supercritical drying and supercritical impregnation with β-carotene. The oil phase was soybean oil with Span® 80 (2 % w/w) as surfactant. The emulsion was heated (75 °C, 3 h) for gelatinization and then cooled (4 °C, 72 h) for retrogradation. The gelled emulsion was subsequently dispersed in an ethanol/water solution, and the particles were separated first with a funnel and then by vacuum filtration. Characterization revealed a mixture of spherical and irregularly shaped particles, often forming small clusters, with diameters ranging from 50 to 100 μm. Araujo et al. (2023, 2024) also produced corn starch aerogels for impregnation with phenolic compounds from passion fruit. However, those studies did not characterize particle size, shape, or release profile.

Alternatively, aerogel powder can be produced by milling or grinding aerogel monoliths as a post-processing step (Manzocco et al., 2021). As shown in Table 1, this straightforward method has been widely applied to starch carriers, likely due to its simplicity.

Wet milling was investigated by Schroeter et al. (2023) as an alternative, top-down approach to produce aerogel particles. Alginate hydrogel and alcogel composite beads were milled in a colloid mill, and after drying, aerogel particles of 50–300 μm with low sphericity were obtained. The effects of process variables and gel properties were also evaluated. Similarly, Z. Wang et al. (2013) produced oxidized starch microgel particles without dedicated milling equipment by forcing the gel through a 1 mm sieve covered with nylon cloth (200 mesh, 0.074 mm). The resulting particles were irregular in shape, with sizes ranging from 10 to 50 μm, although it remains unclear whether the gels were subsequently dried to form aerogel particles.

It becomes clear that a gap remains in the literature regarding the comparison of particle production methods and how processing technology, together with particle size and shape, can affect nutraceutical delivery. In this regard, Baudron et al. (2020) compared the production of starch aerogels as monoliths and microparticles, by the emulsion–gelation technique, but without addressing a specific application.

4.3. Approaches for nutraceutical loading in aerogels

For delivery systems, aerogel synthesis includes an extra step: loading the bioactive ingredient (nutrient). Loading efficiency (LE) and loading capacity (LC), as follows, are two key metrics to assess the success of the impregnation:

$$\text{LE}\ (\%) = \frac{m_N}{m_{N0}} 100 \quad (1)$$

$$\text{LC}\ (\%) = \frac{m_N}{m_A} 100 \quad (2)$$

where m_N, m_{N0} and m_A are the masses of loaded nutrient, nutrient originally added to the formulation, and aerogel, respectively. LE and LC are also relevant to therapeutic dosing, determining the daily mass of carrier needed. Health authorities provide reference nutrient intakes for different populations (*e.g.*, adults by sex) (EFSA, 2019). Given a recommended daily dose and an expected LE, one can back-calculate the amount of nutrient to add during loading; likewise, a target LC allows calculation of the required daily intake of the carrier. Although only a few studies explicitly compute or report a therapeutic dose (Clare et al., 2024; De Marco & Reverchon, 2017), this should be systematically considered to ensure the practical viability of the carrier as a supplement.

The loading step can be introduced at different stages of synthesis, as illustrated in Fig. 7. The first approach (Fig. 7a) involves adding the bioactive compound to the precursor dispersion before the formation of the gel (Zheng et al., 2020). In this way, the compound becomes encapsulated within the gel network during retrogradation (Y. Zhu et al., 2023). For starch systems, this can be done either before or after gelatinization. It is the simplest method but requires the compound to be water-soluble and stable under synthesis conditions such as temperature and agitation. Depending on solubility and loading level, the nutraceutical may also interfere with network formation during retrogradation through steric hindrance (Zheng et al., 2020). In the case of supercritical drying with CO_2, an additional challenge is preventing compound loss during solvent exchange and drying. The extent of loss

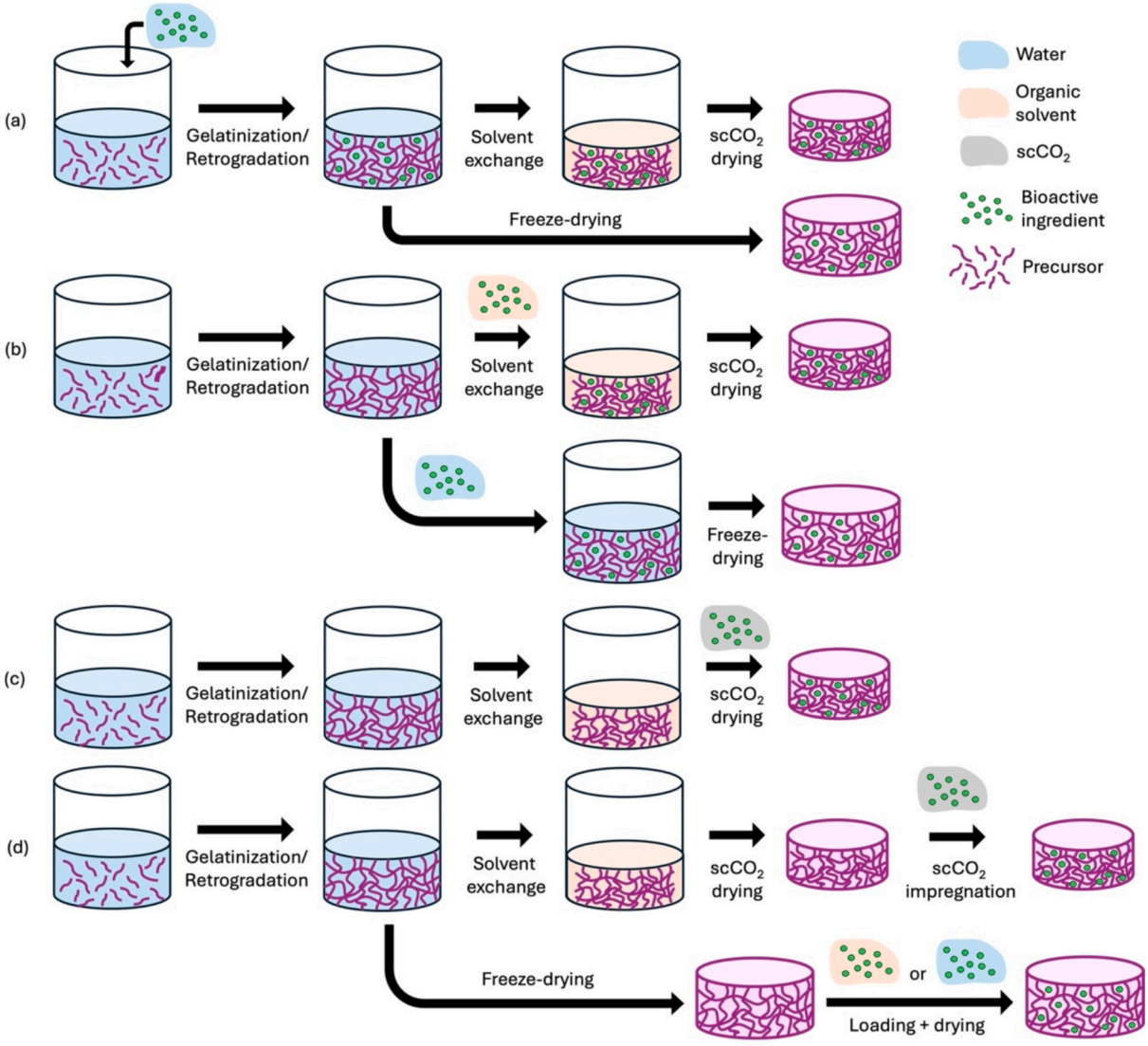

Fig. 7. Methods for loading the bioactive compound into the aerogel matrix: (a) encapsulation after dispersion in precursor solution, (b) wet impregnation; (c) simultaneous impregnation and supercritical drying, (d) impregnation after drying, either by supercritical impregnation or wet impregnation.

depends on the strength and nature of matrix–compound interactions, as well as the solubility of the compound in the organic solvent and $scCO_2$ (García-González et al., 2021).

Several authors, including Zhang, Wang, et al. (2023), H. Li, Lv, et al. (2024), and Yang et al. (2024), have dispersed the bioactive compound in the starch solution before gelatinization (Table 1), all following a similar procedure. Starch is dispersed in water with sodium hexametaphosphate (SHMP) for modification, supplemented with an ethanol solution of the bioactive compound, then agitated and heated for gelatinization, followed by retrogradation and freeze-drying. Ethanol is used to overcome the low solubility of the compound in water. Although dispersion-based encapsulation was proven simple and effective, improving compound stability, the high gelatinization temperature (60–130 °C) can be limiting for heat-sensitive substances.

An alternative is to add the bioactive ingredient to the starch paste after gelatinization and partial cooling, but before retrogradation, as described by Clare et al. (2024, 2025). Clare et al. (2025) detailed the protocol for water-soluble compounds. Combining early encapsulation with freeze-drying helps avoid the nutraceutical losses typically observed during solvent exchange and supercritical drying, achieving loading efficiencies close to 100 %.

Another approach, commonly known as wet impregnation (Fig. 7b), involves immersing the hydrogel in a liquid phase saturated with the bioactive compound, allowing it to gradually diffuse into the porous network (García-González et al., 2021; Selvasekaran & Chidambaram, 2021; Zheng et al., 2020). If the compound is soluble in the alcoholic solvent used for solvent exchange, both steps can be combined by soaking the gel in a solvent, typically ethanol, saturated with the bioactive compound. This is followed by supercritical drying with CO_2, where the solvent is removed and the compound precipitates within the aerogel pores *via* an anti-solvent mechanism (Selvasekaran & Chidambaram, 2021). A key requirement is that the compound must not be soluble in $scCO_2$, otherwise it will be extracted. This method also depends on the diffusivity of the compound into the gel pores, which may lead to slow or incomplete loading, and gradients of concentration in the solid matrix (García-González et al., 2021; Y. Zhu et al., 2023). Alternatively, water or other solvents can be used as the soaking medium, followed by freeze-drying or a separate solvent exchange step.

Soleimanpour et al. (2020) and Alavi and Ciftci (2024a, 2024b) investigated immersion in an ethanol solution containing the food ingredient. They suggested that this approach enables nutraceutical molecules to penetrate the gel's porous structure and subsequently precipitate within the mesopores during supercritical drying, in amorphous or low-crystalline form, thereby enhancing delivery. Soleimanpour et al. (2020) further reported that the reduced crystallinity of genistein after impregnation promoted rapid release in aqueous solution, improving its bioavailability.

The third method (Fig. 7c) involves impregnating the gel during the drying step, using $scCO_2$ saturated with the compound (García-González et al., 2021). In this case, the compound's solubility in $scCO_2$ is a key factor. The dissolved ingredient diffuses into the network pores, and impregnation occurs either through chemical adsorption or by condensation and precipitation upon depressurization (Manzocco et al., 2021; Selvasekaran & Chidambaram, 2021).

Lastly, loading can be carried out after drying (Fig. 7d). In this approach, the aerogel is exposed to a liquid or gas phase containing the dissolved bioactive ingredient, which then precipitates or adsorbs into the pores as the solvent is removed. When aqueous or organic solvents are used, the procedure resembles conventional wet impregnation but is applied to the dry aerogel rather than the gel. However, due to the typically hydrophilic nature of bioaerogels, they tend to collapse or partially dissolve in such media, risking structural damage. An additional drying step is also required after loading, and incomplete solvent removal may compromise food-grade safety (García-González et al., 2021; Manzocco et al., 2021; Y. Zhu et al., 2023). Despite these limitations, wet impregnation of the aerogel with an appropriate solvent still offers advantages, such as the ability to tailor loading capacity, minimize bioactive ingredient consumption, and enable impregnation with a second nutraceutical during the subsequent drying step with $scCO_2$ (Pantić et al., 2024).

Another option for loading dried aerogels (Fig. 7d) is supercritical impregnation, a technique widely applied in drug delivery. In this method, the aerogel – wrapped in a porous mesh or filter paper – and the food ingredient, often placed in an open container, are introduced into the chamber. The wrapping prevents direct contact between the aerogel and the ingredient before dissolution in $scCO_2$. Once the chamber is filled, the dissolved compound diffuses into the aerogel pores (García-González et al., 2021). Loading occurs mainly through two mechanisms: adsorption, where nutraceutical functional groups interact with starch during $scCO_2$ flow (*e.g.*, *via* hydrogen bonding), and precipitation, where the ingredient is physically trapped in the aerogel pores during chamber depressurization (Hatami et al., 2024).

Once again, the solubility of the bioactive ingredient in $scCO_2$ is a critical factor, as it determines the amount that can be impregnated into the carrier. Solubility can be enhanced by adjusting process conditions (*e.g.*, pressure and temperature) or by adding co-solvents such as ethanol (García-González et al., 2021; Hatami et al., 2024; Manzocco et al., 2021). Solubility studies are therefore often carried out as a preliminary step to define optimal impregnation conditions, aiming to maximize solubility – and consequently loading – up to the capacity of the aerogel matrix (De Marco & Reverchon, 2017; Milovanovic et al., 2015; Mottola et al., 2023).

Supercritical impregnation combined with supercritical drying with CO_2, leading to high surface areas, is considered the preferred loading method (see Table 1). Performing supercritical drying and impregnation in sequence also enables a "one-pot procedure," as proposed by Villegas et al. (2019).

Several studies have focused specifically on supercritical impregnation and its optimization (Araujo et al., 2023; Araujo et al., 2024; Dias et al., 2022; Lukic et al., 2022). The influence of process variables such as pressure, temperature, depressurization rate, and cycling has been investigated in relation to both loading capacity and aerogel properties, including surface area (Araujo et al., 2023; Dias et al., 2022). Hatami et al. (2024) further analyzed the process in detail and proposed a mathematical model to describe the precipitation of β-carotene molecules into corn starch aerogels during supercritical impregnation.

Pantić et al. (2024) investigated the incorporation of two compounds – xanthohumol and usnic acid – into the same carrier. Because of their different solubilities, two loading methods were required. After supercritical drying with CO_2, the aerogel was immersed in an ethanol solution of xanthohumol for wet impregnation. The $scCO_2$ process was then applied again, both to dry the wet aerogel and to impregnate it with usnic acid. The authors justified the use of wet impregnation on the dried aerogel, rather than adding xanthohumol during solvent exchange, by the substantial reduction in bioactive ingredient consumption it provided, along with greater control over the loading step. Given the aerogel's soaking capacity, the loading capacity can be tuned by varying the nutrient concentration in the solvent.

4.3.1. *Influence of carrier properties on loading and resulting effects*

The loading capacity is significantly influenced by the properties of the bioactive compound and the loading method, but the matrix properties also play a key role. Among these, the specific surface area of the carrier often constitutes the main factor, as it determines the available interface for adsorption. It is therefore especially important for both wet impregnation and supercritical impregnation. In highly porous materials, the prevalence of mesopores typically results in the high specific surface area characteristic of aerogels.

Alavi and Ciftci (2024b) compared starch aerogels with different amylose contents (25 %, 55 %, 72 %) and found that loading capacity (mg g^{-1}) increased with amylose content, rising by more than half between aerogels with 25 % and 72 % amylose. They attributed this to the

higher surface area, which increases the contact between the matrix and the bioactive ingredient, promoting stronger interactions. To further compare the impregnation performance, the calculation of loading per surface area (mass of nutrient per accessible surface area of aerogel, expressed in mg m^{-2}) can provide additional insight into how effective the occupation of the available surface is. Due to very low densities and high specific surface area of aerogels, normalizing the loading capacity by surface area may help identify saturation limits and evaluate the efficiency of the impregnation. However, up to now, this approach (mg m^{-2}) has not been applied for starch aerogel-based carriers, and it should be interpreted in combination with the standard loading capacity (mg g^{-1}) and with caution, as the metric can be influenced by impregnation mechanism and pore accessibility.

In turn, some studies emphasize porosity as the key contributor. Lukic et al. (2022) reported that higher porosity leads to higher loading capacity, while Alavi and Ciftci (2024a) showed that low bulk density combined with high porosity provides more voids for nutraceutical impregnation. The latter also highlighted the distinct roles of pore types in the carrier: micro- and mesopores contribute to loading and adsorption, whereas macropores facilitate mass transport during release. However, porosity and surface area are not always directly proportional, as materials rich in macropores may exhibit exceptional porosity yet limited surface area. Therefore, porosity must be considered alongside surface area and pore size distribution when evaluating loading capacity.

Along with the structural properties of the aerogel, the affinity between the nutraceutical and the matrix can significantly affect the impregnation. This may explain the higher curcumin impregnation reported by Alavi and Ciftci (2024a) for starch/chitosan composite aerogels, despite their lower surface area compared with neat starch aerogels. Additionally, saturation effects or kinetic limitations, such as restricted diffusion into certain regions of the network, may also influence the maximum amount of compound effectively loaded in the carrier.

In the case of wet and supercritical impregnation methods, adsorption equilibrium is essential to understand the loading mechanism, and optimize its efficiency. Adsorption isotherms determine how the bioactive ingredient concentration in the fluid phase relates to the impregnated quantity, at the equilibrium state, and are specific to the temperature and pressure. Adsorption models from the literature (*e.g.*, Langmuir, Freundlich and Temkin isotherms) can then be fitted to experimental data to evaluate the nutrient affinity for the matrix, understand the adsorption mechanism, and predict the maximum loading capacity. Additionally, adsorption kinetics can be assessed to evaluate the rate of impregnation and explore the diffusion mechanisms, which can affect the distribution of the compound in the carrier. Kinetic models (*e.g.*, pseudo-first-order and pseudo-second-order) can also be applied to experimental data. Despite their importance, thermodynamic and kinetic studies are still rare in the nutraceutical delivery field (De Marco & Reverchon, 2017; Soleimanpour et al., 2020).

On the other hand, nutrient impregnation also alters the aerogel matrix, typically evaluated through morphological and textural properties. As shown in Table 1 (for studies reporting such data), the specific surface area consistently decreases after nutraceutical incorporation using supercritical and/or wet impregnation. However, the extent of this reduction varies widely, from about 4 % (De Marco & Reverchon, 2017) to 45 % (Pantić et al., 2024).

Dias et al. (2022) reported that β-carotene molecules penetrate the aerogel pores during supercritical impregnation, occupying the available spaces and reducing surface area, pore volume, and pore size. Araujo et al. (2023) observed a 19 % decrease in surface area but noted that the overall aerogel morphology remained mostly unaffected, as shown by SEM images and nitrogen adsorption/desorption profiles. They attributed the reduction to phenolic compounds impregnated in the mesopores. In a subsequent study, Araujo et al. (2024) achieved a smaller decrease of 8 %. By contrast, Pantić et al. (2024) reported reductions of 34–45 %, although SEM images again indicated that the aerogel structure was mostly preserved, even though wet impregnation after drying was applied.

In the case of encapsulation after dispersion (Fig. 7a), Zhang, Wang, et al. (2023) observed that β-carotene impregnation caused the loss of the aerogel's porous structure. A similar effect was reported by H. Li, Lv, et al. (2024) after cannabidiol impregnation, attributed to the use of ethanol in the loading process. Ethanol promotes the formation of amorphous starch, which establishes non-covalent interactions with cannabidiol, leading to a disrupted microstructure. Likewise, Zhang, Wang, et al. (2023) concluded that ethanol addition to the starch paste produced an amorphous network that encapsulated β-carotene through non-specific binding.

In the case of encapsulation by dispersion followed by freeze-drying, conflicting results have been reported regarding the effect of nutrients on the specific surface area. H. Li, Lv, et al. (2024) observed a 33 % decrease with cannabidiol incorporation, whereas Yang et al. (2024) found a higher surface area in aerogels loaded with procyanidin, likely because the compound inhibited ice crystal growth during freeze-drying.

Overall, supercritical impregnation preserves the aerogel's porous structure better than encapsulation after dispersion. In the latter, the structure forms around the nutrient and is therefore more affected by it. Clare et al. (2024) showed that this effect depends on loading quantity: the carrier with a small amount of folic acid (0.390 ± 0.003 wt%) maintained a structure similar to pure starch, while high iron loading (11.05 ± 0.01 wt%) disrupted reticulation, producing a more fragile matrix (Fig. 8). This fragility also led to faster iron release under intestinal conditions, as the carrier degraded more easily.

In contrast, when supercritical impregnation is applied after the porous network is fully developed, the structure is preserved, likely due to the absence of capillary forces in the supercritical state. It is worth noting that, even with surface area reductions of up to 45 %, aerogels produced by supercritical drying combined with supercritical impregnation still retain higher surface areas than those obtained by encapsulation followed by freeze-drying, as shown in Table 1.

Table 3 summarizes the main features of the three combined synthesis and loading strategies, but comparisons remain highly dependent on the type of nutraceutical. Although several methods have been tested individually in the studies reviewed, the literature still lacks systematic comparisons of loading methods applied to the same nutraceutical–carrier system. Such studies would provide valuable insights into how the loading method affects parameters like LC and LE, as well as the properties of the loaded aerogels, and could serve as a basis for selecting the most suitable method.

As shown in Table 3, the choice of a loading method strongly depends on the nutraceutical's properties, as these determine its solubility in water, organic solvents, and $scCO_2$, as well as its affinity for the matrix. The limitations of experimental techniques can be mitigated by complementing them with molecular simulation, particularly for predicting the interactions involved.

4.4. Starch digestion and nutraceutical release

Most nutraceuticals are absorbed in the small intestine. Therefore, oral administration is the preferred route, and the carrier must remain stable throughout the gastrointestinal tract until reaching the target site, where the nutraceutical is released (Gonçalves et al., 2018). It is essential to evaluate both carrier integrity and bioactive compound bioavailability throughout the gastrointestinal tract to determine release efficiency. For starch carriers, *in vitro* tests can be performed to assess two interconnected processes: starch digestibility, measured by the degree of digestion, and the release of the nutraceutical over time in the digestive environment (Brodkorb et al., 2019; Sun et al., 2023).

In vitro digestion methods are classified into static and dynamic approaches. The latter are usually more complex and costly, simulating

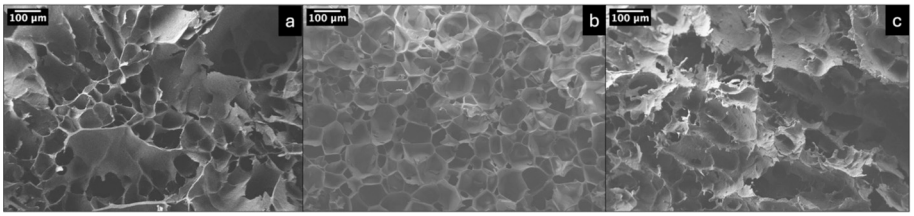

Fig. 8. SEM images of freeze-dried starch carriers: (a) unloaded; (b) loaded with folic acid; (c) loaded with iron. Reproduced from Clare et al. (2024) with permission from Elsevier.

Table 3
Comparison of main strategies for impregnation of starch-based nutraceutical delivery systems.

	Encapsulation	Wet impregnation	Supercritical impregnation
Impregnation protocol[(1)]	1. Dispersion of BI + starch in water, before or after gelatinization 3. Retrogradation 4. Freeze-drying	1. Immersion of hydrogel in solvent saturated with BI, during solvent exchange 2. $scCO_2$ drying	1. $scCO_2$ drying 2. Impregnation of the dried aerogel with the BI dissolved in $scCO_2$
Mechanism of impregnation	• Encapsulation of BI within the gel as it is formed	• Diffusion of BI (in liquid phase) into the porous network • BI adsorption or precipitation upon depressurization during drying step	• Diffusion of BI (dissolved in $scCO_2$) into the porous network • BI adsorption or precipitation upon depressurization
Restrictions for BI	• Soluble in water • Withstand the synthesis conditions, *e.g.*, temperature and agitation	• Soluble in the new solvent • Not soluble in $scCO_2$, to avoid extraction during drying	• Soluble in $scCO_2$
Advantages	• Simple method • Avoids the use of organic solvent • High LE • High LC (SSA is not a limiting factor)	• Integration with solvent exchange step • Precipitation of ingredient in an amorphous/low crystalline form that is more bioavailable	• Better preservation of the porous network • Precipitation of ingredient in an amorphous/low crystalline form that is more bioavailable
Disadvantages	• BI can hinder reticulation and the proper formation of the porous network • BI degradation during processing steps	• Use of organic solvents • Often slow, non-homogeneous and/or incomplete loading • Implies previous studies on adsorption isotherms • LC depends on SSA and solubility	• Use of organic solvents • Two cycles with $scCO_2$ (cost and safety issues) • Implies previous studies on adsorption isotherms • LC depends on SSA and solubility

[1] Integrated with the synthesis protocol. BI – bioactive ingredient. $scCO_2$ – supercritical CO_2. LE – loading efficiency. LC – loading capacity. SSA – specific surface area.

real-time variations in the gastrointestinal tract, such as pH and enzyme concentration. In contrast, static models rely on electrolyte solutions with fixed concentrations and pH values to represent each gastrointestinal fluid (saliva, gastric, and intestinal). The stages can be performed sequentially to better mimic human digestion, being contact time, temperature, and agitation considered key factors.

Several recent studies on starch-based aerogel carriers do not include delivery tests (Araujo et al., 2023; Araujo et al., 2024; Dias et al., 2022; Lukic et al., 2022), although some authors have begun to emphasize their importance (Pantić et al., 2024). When release protocols are applied, they often use only phosphate-buffered saline solutions to mimic intestinal conditions (De Marco & Reverchon, 2017; Mottola et al., 2023), both gastric and intestinal phases (Soleimanpour et al., 2020; Yang et al., 2024), or the full gastrointestinal tract with saliva, gastric, and intestinal fluids (H. Li, Lv, et al., 2024; Zhang, Wang, et al., 2023). In addition, most studies focus exclusively on measuring nutraceutical release rather than starch digestibility, with few exceptions (Clare et al., 2024; Ubeyitogullari et al., 2019).

It is clear that the complexity of the protocols used varies greatly, which hinders comparison. To address this issue, INFOGEST provides a standardized protocol for static *in vitro* simulation of gastrointestinal digestion, suitable for evaluating micronutrient release from the food matrix. The method was designed to mimic digestion of any food system and has been validated against *in vivo* physiological data (Brodkorb et al., 2019). The conditions for a general simulated digestion study for starch-based samples are summarized in Table 4. To date, only a few reports on starch have used adapted versions of the INFOGEST protocol (Alavi & Ciftci, 2024a, 2024b; Ubeyitogullari et al., 2019).

The first stage of digestion (the mouth) is usually negligible due to the short residence time, although salivary amylase initiates starch hydrolysis by cleaving α-1,4-glucosidic bonds. In the stomach, the low pH inhibits salivary amylase, and starch remains relatively stable. More substantial digestion occurs in the small intestine: pancreatic amylase hydrolyzes α-1,4-glucosidic bonds, while maltase and sucrase, which can cleave both α-1,4 and α-1,6 bonds, further convert the resulting products into glucose (Boldrini, 2023; Sun et al., 2023).

Based on digestion rate and glucose release, starch can be divided into three categories. Rapidly digestible starch releases glucose immediately, whereas slowly digestible starch promotes a gradual increase in blood glucose. The fraction not digested in the small intestine of healthy individuals is known as resistant starch, which behaves as dietary fiber. Compared with the other types, resistant starch offers additional health benefits, including probiotic effects, lower glucose release, and reduced caloric value. Resistant starch can be found as native granules or as retrograded or chemically modified starch (Boldrini, 2023; Jiali et al., 2024).

When it comes to starch aerogel carriers, it is also important to consider the impact of the aerogel structure on the digestion rate, alongside the intrinsic starch digestibility. The retrogradation step in the synthesis of starch aerogels contributes to the increase in resistant starch content, delaying digestion. On the other hand, the highly porous network, combined with the high surface area, can facilitate release. When comparing the release of quercetin from starch aerogels, Mottola et al. (2023) reported a fast initial burst of 70–80 % within 20 min for corn starch aerogels, whereas the initial release from potato aerogels was much slower, reaching 80 % only after 40 min. The authors attributed the faster release to the higher surface area, while in the latter case the ingredient is retained within the less porous structure of the network, slowing release. Although fast release can be advantageous for certain nutraceuticals, it is essential that the highest release occurs only

Table 4
Simulated digestion fluid compositions and protocol conditions indicated by the INFOGEST model (Brodkorb et al., 2019; Zhou et al., 2023). All solutions are aqueous-based.

Digestion stage composition	Ratio	Mouth Carrier to simulated saliva fluid: 1:1 (w/w); add extra water to obtain paste-like consistency	Stomach Oral bolus (from previous stage) to simulated gastric fluid: 1:1 (v/v)	Intestine Gastric chyme (from previous stage) to simulated intestinal fluid: 1:1 (v/v)
	Total digesta (final volume at each stage)	2*v*	4*v*	8*v*
Simulated digestion fluid composition / mmol L^{-1}	KCl	15.1	6.9	6.8
	KH_2PO_4	3.7	0.9	0.8
	$NaHCO_3$	13.6	25	85
	NaCl	–	47.2	38.4
	$MgCl_2(H_2O)_6$	0.15	0.12	0.33
	$(NH_4)_2CO_3$	0.06	0.5	–
	HCl	1.1	15.6	8.4
	$CaCl_2(H_2O)_2$ [1]	1.5	0.15	0.6
Enzyme activity (in total digesta) / U mL^{-1}	Salivary amylase	75	–	–
	Pepsin	–	2000	–
	Gastric lipase	–	60	–
	Amylase in pancreatin	–	–	200
Bile salts (in total digesta) / mmol L^{-1}		–	–	10
pH		7.0	3.0 [2]	7.0 [3]
Temperature / °C		37	37	37
Incubation time / min		0–2	120	120

[1] Add immediately before the test, to avoid precipitation.
[2] Adjust the pH with HCl 5 mol L^{-1}.
[3] Adjust the pH with NaOH 5 mol L^{-1}.

in the intestine. In this context, it is necessary to find a compromise between faster release and higher loading, both of which depend on surface area.

Moreover, it is consistently reported that the use of an aerogel carrier improves nutraceutical bioavailability, especially for ingredients with low water solubility due to high hydrophobicity and/or crystalline form (Alavi & Ciftci, 2024b; H. Li, Lv, et al., 2024; Mottola et al., 2023; Ubeyitogullari et al., 2019). For impregnation, the nutraceutical must first be dissolved in the solvent or in $scCO_2$, and the high surface area combined with the small pores of the network prevents recrystallization of the ingredient after the solvent/$scCO_2$ is removed. As a result, the nutraceuticals in a less crystalline and/or smaller-size form are more easily solubilized in intestinal fluid, thereby increasing bioavailability (Mottola et al., 2023; Ubeyitogullari et al., 2019). The hydrophilicity of starch also plays a key role by facilitating the penetration of the medium into the matrix and the dissolution of the nutraceutical (Soleimanpour et al., 2020).

Quantifying nutraceutical release is then essential for characterizing the carrier. Modeling the release profiles with kinetic models (*e.g.*, pseudo-first-order, pseudo-second-order and Korsmeyer-Peppas) can help identify the predominant release mechanism. In diffusion-dominated release, the aerogel's porous structure remains stable, and the transport of nutraceutical through the pores and into the gastrointestinal medium is governed by concentration gradients. Conversely, if starch is rapidly digested, the aerogel structure collapses, and its disruption directly dictates the nutraceutical release with sharper profiles.

Therefore, the integrity of the carrier throughout the gastrointestinal tract and the release of the nutraceutical are strictly related. Since nutraceuticals are usually absorbed in the intestine, it is important to ensure that the initial burst is delayed until reaching this stage or, at least, that the release rate is controlled. Particularly in cases where release is not diffusion-dominated, specific strategies can be applied to ensure targeted delivery by minimizing starch degradation and digestion (Sun et al., 2023). Physical, chemical, and enzymatic modifications can increase resistant starch content to reduce digestion and help overcome other starch limitations. In recent years, several reviews have examined these modifications in detail, discussing methods, resulting properties, and application as delivery systems (Garcia et al., 2020; Jiali et al., 2024; Karma et al., 2022; Labelle et al., 2020; Tian et al., 2022).

In addition to increasing resistant starch content, chemical modification can also enhance carrier performance by improving its stability and its interaction with the nutraceutical through the incorporation of functional groups. Each D-glucopyranosyl unit of starch has three hydroxyl groups available for reaction (at C2, C3, and C6; Fig. 1), and the extent of reaction is expressed as the degree of substitution, *i.e.*, the average number of hydroxyl groups replaced per unit (Boldrini, 2023). Common chemical modifications include oxidation, esterification, etherification, and cross-linking, achieved with different reactants and conditions (Boldrini, 2023; Garcia et al., 2020). Karma et al. (2022) highlighted the use of GRAS organic acids – such as citric, succinic, stearic, and malic acid – as a promising approach for nutraceutical carriers due to their inherent biocompatibility.

As shown in Table 1, some authors have already explored chemical modification of starch aerogels to improve nutraceutical delivery. Zhang, Wang, et al. (2023) prepared corn starch aerogels cross-linked with SHMP and successfully encapsulated β-carotene in the amorphous matrix through non-specific interactions. The carrier effectively protected the bioactive ingredient, enhancing its bioavailability and its stability under UV-light irradiation. Yang et al. (2024) applied the same SHMP modification to rice, corn, and wheat starches; after screening, SHMP-modified wheat starch was selected to encapsulate procyanidins, through a similar mechanism. This carrier also improved compound stability and enabled targeted release in the final stage of simulated digestion. Thus, it is also frequently reported that the modified starch aerogels can enhance compound stability in addition to improving bioavailability – both intrinsic challenges in nutraceutical delivery.

The addition of other biopolymers to obtain composite materials has also been attempted. Alavi and Ciftci (2024a) used chitosan in different concentrations (0, 0.5 and 0.75 % w/w) to modulate the final aerogel properties. The highest loading capacity was observed for the composite of corn starch and 0.5 % of chitosan, attributed to the higher meso- and microporosity and lower density, but it may also be related to favorable interactions between the matrix and the nutrients. The addition of chitosan also enhanced the bioaccessibility and antioxidant activity of curcumin. In another study, Pantić et al. (2024) incorporated nanocellulose, as cellulose nanocrystals or bacterial nanocellulose, into the starch matrix, thus significantly improving its carrier properties, such as

surface area, adsorption capacity and stability.

It is important to acknowledge that incorporating these aspects into carrier design is essential for enhancing delivery efficiency and efficacy. To achieve this, a comprehensive strategy based on a complete simulated digestion study using a standardized protocol, followed by modeling of the release profile, is recommended. The analysis should consider starch digestion and nutraceutical release in an integrated manner, modifying the matrix accordingly – either to increase resistant starch content or to improve interactions with the nutraceutical. Current studies still lack this engineering-oriented perspective, but it should be a key priority for future research in the field.

In this context, molecular modeling can help to reduce reliance on traditional trial-and-error experimentation by providing insights into the interactions between the nutraceutical and the matrix, predicting system behavior under simulated digestion conditions, and elucidating how different modification strategies may influence these outcomes.

4.5. *Safety and regulatory framework of starch aerogels*

Starch has long been an essential part of the human diet, mainly from potato, rice, maize, and wheat. It is non-allergenic, non-toxic, abundant, and inexpensive, making it widely used in the pharmaceutical industry, especially in oral medicines as excipients such as binders, filler-diluents, disintegrants, and glidants in tablet formulations. The FDA classifies starch as GRAS, and several starch excipients —including native corn starch and chemically or physically modified starches — are FDA-approved for pharmaceutical use (F. Zhu, 2019; Garcia et al., 2020). Starch from various plant sources is also listed as a "safe excipient" in the European Pharmacopoeia, published by the European Directorate for the Quality of Medicines and HealthCare (EDQM, 2023).

Regarding the safety of starch-based aerogels for human consumption, clear regulations for their use in the food industry are still lacking. The Novel Foods Regulation (EU Regulation 2015/2283) defines "novel food" as any food not consumed within the European Union (EU) before 1997 (EPCEU, 2015). However, most biopolymer aerogels are made from polymers long recognized as safe and already present in the human diet. This raises the question of whether such materials should fall under the scope of this regulation. The two main points of contention are the production methods and the final properties of the material. While freeze-drying is well established in the food industry, other techniques – such as supercritical impregnation – remain at the research stage.

It can also be argued that the large surface area and porous structure of aerogels are intentionally engineered physicochemical properties that make them significantly different from the original biopolymer. As such, the need for specific authorization for using biopolymer aerogels in food remains a matter of debate (Manzocco et al., 2021). Further studies on the toxicity and biocompatibility of starch aerogels are necessary to support proper classification and regulation by authorities, and to enable their commercial use as nutraceutical carriers.

5. Molecular simulation in nutraceutical delivery

The growing interest in molecular simulation lies in its ability to explore matter at the atomic and molecular scale, offering insights often inaccessible through experiments. Various simulation methods exist, each balancing accuracy, detail, and computational cost differently. The choice depends on the study's goals, the level of detail needed, and the computational resources available.

At its foundation, molecular simulation uses particle-based models to represent molecular systems, generating trajectories based on physical principles. The theoretical framework used to describe these systems is typically based on either quantum mechanics (QM) or molecular mechanics (MM) (Jensen, 2017; Braun et al., 2019).

QM methods describe how particles behave at the quantum level by explicitly treating electrons, therefore essential for studying electronic structure and chemical reactivity. These approaches are typically divided into two main categories: *ab initio* methods, which rely solely on quantum theory; and semi-empirical methods, which simplify calculations by incorporating experimental data. A widely used alternative to pure *ab initio* methods is density functional theory (DFT), which offers an attractive balance between accuracy and computational efficiency, making it ideal for calculating equilibrium properties such as molecular geometries, binding energies, and reaction profiles. Both *ab initio* and DFT methods are frequently used to study structural, energetic, and spectroscopic properties with high precision (Jensen, 2017; Braun et al., 2019).

Molecular mechanics (MM), in contrast, simplifies the system by representing atoms – or groups of atoms – as charged point masses. Interactions are described using empirical force fields, which account for bonded terms (bonds, angles, torsions) and non-bonded terms (electrostatic, van der Waals), and heavily influence accuracy. These models assume a fixed molecular structure – meaning that chemical bonds do not break or form during the simulation (Jensen, 2017; Braun et al., 2019).

A widely used MM-based technique is molecular dynamics (MD). Classical MD simulates how particles move over time, allowing the study of how molecules behave, interact, and evolve under different conditions. MD enables the calculation of a broad range of structural, thermodynamic, and dynamic properties, including diffusion rates, conformational flexibility, and interaction patterns. However, simulations become more demanding as system size and simulation time increase. Systems with slow molecular dynamics, such as those involving biopolymers like starch, require longer simulations to capture meaningful behavior. It is therefore important to find a balance between system complexity, simulation length, and computational cost, while ensuring that enough of the system's behavior is sampled to draw robust conclusions (Braun et al., 2019; Y. Wang et al., 2022).

In the context of nutraceutical delivery, molecular simulation is a powerful tool to explore how bioactive compounds interact with carrier matrices, how they behave under different environmental conditions, and how they may be released and absorbed in physiological settings. These insights are particularly valuable when designing delivery systems with targeted release, stability, and efficacy in mind. Fig. 9 summarizes the molecular simulation methods most relevant to this review.

Computer-aided molecular modeling and simulation is still underexploited in food research when compared to other fields like pharmaceutical applications (Carpio et al., 2021; Zhang, Li, et al., 2023). Recently, Zhang, Li, et al. (2023) emphasized the importance of studying molecular interactions in food systems to better understand underlying mechanisms. They reviewed available characterization techniques and highlighted the growing potential of computational tools in this area.

Y. Wang et al. (2022) provided a comprehensive review of molecular simulation in food science, with particular focus on carbohydrates. Their work demonstrates how molecular simulation can reveal features that are difficult or even impossible to uncover experimentally, including mechanisms underlying interactions and structural properties.

Similarly, Carpio et al. (2021) emphasized the value of MD simulations in nutraceutical research, particularly for studying how

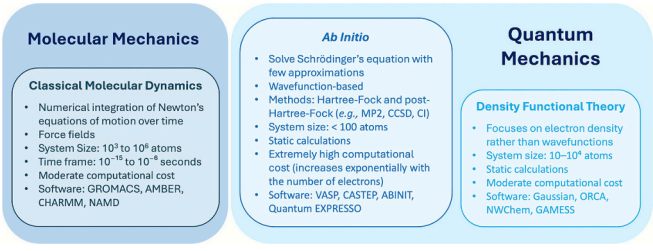

Fig. 9. Main features of the molecular simulation methods relevant to this review, including classical molecular dynamics, *ab initio* and density functional theory.

interactions between molecules evolve over time under varying conditions such as temperature, pressure, and pH. While these reviews outline the broader role of molecular simulation in food and nutraceutical science, the present review aims to explore this perspective within the specific context of designing starch aerogel carriers.

However, due to their complex porous structures and high atom counts, simulating aerogels remains computationally challenging. Patil et al. (2021) reviewed the use of computational methods for modeling and simulating aerogels derived from different precursors. Silica aerogels are the most frequently studied, while biopolymer-based aerogels – including those derived from cellulose – have received far less attention. To date, no studies have modeled starch aerogels as full 3D networks using molecular simulation. Therefore, although this review focuses on starch aerogels for nutraceutical delivery, this section includes any starch–nutraceutical carrier system where molecular simulation has been applied.

In nutraceutical delivery, MD simulations help assess interactions between the matrix and the nutrients, offering insights that support carrier design. DFT calculations can complement this by characterizing the nutraceuticals at a theoretical level and refining force fields for MD when necessary.

Feng et al. (2015, 2016) reviewed the use of molecular simulation – particularly MD – for studying carbohydrates. They discussed the most common software, protocols, and force fields used for carbohydrate modeling, as well as the typical research targets such as structural analysis and interaction mechanisms with other molecules. Table 5 updates this overview by summarizing recent studies that used MD to explore systems involving starch and bioactive compounds for food-related applications. Among them, only Clare et al. (2024) explicitly explores starch aerogels as nutraceutical carriers.

Most of the publications summarized in Table 5 use MD to track interaction dynamics – especially complexation phenomena between the starch-like molecules and nutraceuticals – that can be highly valuable for carrier design. All simulations were performed in aqueous phase, and several metrics were used to analyze how the system evolved and to characterize the interactions involved. Across the selected studies, non-covalent interactions dominate – notably hydrogen bonds (Chen, Chen, et al., 2020; Feng et al., 2020; X. Li, Dai, et al., 2024; X. Li, Li, et al., 2024), hydrophobic effects (X. Li, Dai, et al., 2024; X. Li, Li, et al., 2024), and electrostatic interactions (Chen, Huang, et al., 2020).

A noticeable trend is the integration of MD with experimental techniques, which allows more robust system characterization and validation of simulation results. For example, the formation of a complex between starch and dodecyl gallate was predicted to be favorable by MD simulation, and its conformation was later validated by UV–vis spectroscopy, calorimetric, and crystalline measurements (Chi et al., 2018).

Moreover, the ability to vary conditions such as temperature in MD simulations can help predict how the nutraceutical influences the synthesis and, consequently, the properties of the starch aerogel. Chen, Chen, et al. (2020) evaluated the effect of tea polyphenols on the gelatinization and retrogradation of starch. They simulated a heating program (10 ns, from *ca.* 0 to 340 K) followed by a cooling program (10 ns, from 370 to 277 K) and concluded that the presence of the nutraceutical interfered with the interaction and arrangement of polymer chains through different mechanisms in each case. In carrier design, such analyses can be useful for determining whether encapsulation after dispersion in the precursor solution is viable and whether the nutraceutical should be added before or after gelatinization, ultimately serving as a criterion for selecting the loading method.

Furthermore, MD simulation can be used to explain or predict aspects of delivery. Clare et al. (2024) interpreted the release profile of folic acid based on its interactions with amylose observed in MD simulations. Similarly, Xie et al. (2024) applied MD to gain molecular-level insight into the release mechanism of pH-responsive starch nanocapsules by varying the simulated pH and the protonation state. However, it is important to note that the real gastrointestinal environment is far more complex, and its representation in MD simulations through pH variations is only weakly realistic.

System size is another significant challenge in MD studies. Due to the extremely high computational demand of polymeric systems, most simulations simplify the starch matrix, often modeling it as a short

Table 5
Main food-related publications involving MD simulation of systems with starch-type molecules and bioactive compounds.

System	Main research topic	Software/ package	Force field (for starch and nutraceutical)	Experimental component	Main interactions	Reference
Amylose (V-type helical structure) + fatty acids (linoleic and stearic)	Complexation and conformational changes	GROMACS	GROMOS $56A6_{CARBO\_R}$	No	H-bonds	Cheng et al. (2018)
Amylose chain (35 resid.) + DG	Complexation	AMBER	Amylose: GLYCAM-06j-1; DG: AMBER (GAFF)	Yes	NA	Chi et al. (2018)
Two parallel short-chain glucose (3 left-handed helixes of 18 resid. each) + tea polyphenols (*e.g.*, EGCG)	Interaction mechanism	AMBER	Starch: GLYCAM-06j-1; EGCG: AMBER (GAFF)	Yes	H-bonds	Chen, Chen, et al. (2020)
Single amylose (55 resid.) and double helix (each chain: 25 resid.) + trilinolenin	Complexation (interaction forces, conformation and stability)	AMBER	GLYCAM-06 and GAFF	No	Van der Waals, electrostatic	Chen, Huang, et al. (2020)
Debranched starch (12 resid., with 6-fold left-handed amylose helix) + curcumin	Interaction mechanism	AMBER	Starch: GLYCAM-06; Curcumin: AMBER	Yes	H-bonds, water bridges	Feng et al. (2020)
Amylose (26 resid.) + egg yolk lipids (cholesterol, POPC and triglyceride)	Complexation	GROMACS	CHARMM36	No	H-bonds, hydrophobic	Sang et al. (2021)
β-cyclodextrin/amylose (36 resid.) + caffeine	Release behaviors of caffeine	GROMACS	GROMOS $56A6_{CARBO\_R}$	Yes	H-bonds, electrostatic, hydrophobic,	Shao et al. (2021)
Amylose (20 resid.) + folic acid	Interaction mechanism	GROMACS	CHARMM36	Yes	H-bonds	Clare et al. (2024)
V7-type amylose (35 resid. with 7-fold left-handed helix) + curcumin	Complexation and stability mechanism	GROMACS	GLYCAM06	Yes	H-bonds, hydrophobic	X. Li, Dai, et al. (2024)
V7-type amylose (35 resid. with 7-fold left-handed helix) + resveratrol	Complexation and stability mechanism	GROMACS	GLYCAM06	Yes	H-bonds, hydrophobic	X. Li, Li, et al. (2024)
RGD peptide-grafted carboxymethyl starch and cationic quaternary ammonium starch + ovalbumin	Release mechanism of ovalbumin in different pHs	NA	AMBER18 (GLYCAM_06j-1 and GAFF)	Yes	H-bonds, electrostatic	Xie et al. (2024)

H-bonds – hydrogen bonds. DG – dodecyl gallate. EGCG – epigallocatechin gallate. NA – data not available. POPC – 1-palmitoyl-2-oleoyl-*sn*-glycero-3-phosphocholine. RGD – arginylglycylaspartic acid.

amylose chain. In the case of starch aerogels, system size becomes even more problematic because the porous network is fundamental to the carrier's properties. Therefore, although MD simulations can provide valuable insights into the delivery system, they are still far from capturing a complete model that reflects all its complexities.

X. Li, Dai, et al. (2024) and X. Li, Li, et al. (2024) used molecular docking to investigate the interactions between amylose and curcumin, and amylose and resveratrol, respectively. Molecular docking is a computational approach used to predict the optimal orientation and binding affinity between two interacting molecules – typically a small ligand and a larger molecule, such as a protein (Jensen, 2017). In these studies, docking was applied to amylose–nutraceutical complexes to identify likely binding sites and estimate binding energies (X. Li, Dai, et al., 2024; X. Li, Li, et al., 2024).

DFT offers a more detailed approach to studying the structure and behavior of the interactions between starch molecules and nutraceuticals. Although still limited in number, existing studies consistently report that these interactions are predominantly non-covalent. DFT is particularly useful for elucidating the mechanisms and characteristics of such interactions (Hao, Xu, et al., 2024).

Wu et al. (2022) combined DFT calculations with experimental methods to study interactions between gelatinized/hydrolyzed wheat starch and trans-resveratrol. Their results showed that complex formation enhances the stability and bioavailability of the bioactive compound. Additionally, the presence of the nutraceutical may both inhibit starch hydrolysis – facilitating target delivery – and reduce the glycemic index by interacting with the hydrolyzed products.

Similar combined approaches have been reported for other systems, including high amylose corn starch–ferulic acid (Hao, Han, et al., 2024), maize starch–L-theanine (Hao, Hu, et al., 2024), and corn starch–lauric acid (Hao, Xu, et al., 2024). These studies have examined how complexation affects starch digestibility, offering mechanistic insights into the role of the bioactive compounds. In particular, an increase in the short-range ordering of starch due to the presence of helical structures and hydrogen bonds led to greater resistance against enzymatic digestion (Hao, Xu, et al., 2024).

Zhang et al. (2024) also employed DFT to study the interaction between nobiletin and rice starch, optimizing the molecular structures and calculating vibrational spectra of the individual components and their complex. Experimental validation confirmed that the hot-melt extrusion-assisted incorporation of nobiletin enhances starch's nutritional value and functional properties, particularly by slowing down its digestion. Therefore, DFT has great potential for guiding starch modification toward enhanced digestion resistance and effective nutraceutical binding, thereby ensuring target delivery.

In summary, molecular simulation has primarily been applied to investigate starch–nutraceutical complexation, focusing on the stability of the resulting complexes and the nature of the interactions involved. Although still an emergent field, this work demonstrates the significant value of computational tools in guiding the design of nutraceutical carriers, offering insights that complement and enhance traditional experimental approaches.

As a final note, it is worth mentioning that the advent of artificial intelligence and the current momentum in quantum-computing research herald a new paradigm in the realm of molecular simulation. Although this is not the focus of the present review, interested readers may refer to the growing body of published information on the topic – Keith et al. (2021), Unke et al. (2021), Mehdi et al. (2024), J. Chen et al. (2025) and Poma et al. (2025) on machine learning and related topics, and Cao et al. (2019), Ollitrault et al. (2021) and Patel et al. (2025) on quantum computing. The suggested references are broad in nature and do not specifically address starch, but provide valuable advances that can be explored in future research.

6. Final remarks and future perspectives

The appeal of starch aerogels as nutraceutical carriers lies in combining the unique properties of aerogels – high porosity and surface area – with the biocompatibility, abundance, and low cost of starch. Together with their versatility and simple production, these carriers offer great potential to enhance the stability and bioavailability of nutraceuticals.

The production of starch aerogels relies on two key starch transformations: gelatinization and retrogradation. While monoliths are easily obtained, carrier morphology plays a crucial role in bioactive compounds release. Spherical particles are most suitable for delivery but are often overlooked. In contrast, the choice of loading method usually depends on the nutraceutical's properties. The most common approach is supercritical drying with CO_2 followed by supercritical impregnation, which yields high surface areas and good loading capacities.

Although the synthesis of starch aerogels has been studied and optimized, few studies adjust production with the final application in mind. Tuning carrier properties throughout the production steps remains largely unexplored. To advance the field, systematic comparisons of loading methods and particle production techniques are needed. The literature also lacks a practical approach to carrier design – for example, assessing loading capacity against the recommended daily dose would help evaluate the aerogel's viability. Co-delivery of two or more nutraceuticals is also emerging as a research trend. Possible synergistic effects could improve efficacy, enhance absorption, reduce the required dose, and simplify supplementation by combining multiple nutrients in a single formulation (Clare et al., 2024; Sun et al., 2023).

Simulated digestion studies are essential to understand carrier degradation and nutraceutical release under gastrointestinal conditions. However, standardized procedures should be used to ensure fair comparisons and reliable conclusions. To delay degradation and improve delivery, starch aerogel properties can be enhanced through starch modification or by developing composite systems.

Interactions between the matrix and nutrients – and between nutrients in co-delivery systems – are a critical aspect of carrier design. As these processes often occur at the nanoscale, they are difficult to fully characterize experimentally. Molecular modeling offers a powerful alternative, enabling early screening of combinations and reducing trial-and-error experiments – for example, by comparing the affinity of different modified starches for a given nutraceutical. It also allows simulation of system dynamics in aqueous solution, under varying temperature and pH, to mimic gastrointestinal conditions. In short, computational tools can help rationalize carrier design and significantly enhance nutraceutical delivery using starch-based aerogels.

Current literature also lacks thorough characterization of the delivery system, which is essential for practical application. The stability of both the nutraceutical and the carrier must be evaluated to determine suitable packaging and storage conditions. This includes testing the effects of temperature, oxygen, and humidity over time on the system's physical and chemical properties. Additionally, assessing the toxicity of the carrier – particularly in relation to its aerogel morphology – is crucial to ensure its safety and applicability.

The viability of scaling up is another key aspect for future research. Some methods, like freeze-drying, are already well established in the food industry, making certain production routes – such as encapsulation followed by freeze-drying – more accessible. Although scaling up supercritical technology is a growing trend in aerogel research, several challenges still need to be addressed.

Significant progress has been achieved in the lab-scale synthesis of starch aerogels for nutraceutical delivery, but further work is needed to optimize carrier design and ensure future applicability and market potential.

Abbreviations

AP	Amylopectin
AM	Amylose
DFT	Density functional theory
DG	Dodecyl gallate
EDQM	European Directorate for the Quality of Medicines and healthcare
EFSA	European Food Safety Authority
EGCG	Epigallocatechin gallate
EU	European Union
FDA	U.S. Food and Drug Administration.
FTIR	Fourier-Transform Infrared
GRAS	Generally Recognized as Safe
LE	Loading efficiency
LC	Loading capacity
MD	Molecular dynamics
NA	Data not available
POPC	1-palmitoyl-2-oleoyl-*sn*-glycero-3-phosphocholine
RGD	arginylglycylaspartic acid
$scCO_2$	Supercritical CO_2
SEM	Scanning Electron Microscopy
SHMP	Sodium Hexametaphosphate
UA	Usnic Acid
XH	Xanthohumol
XRD	X-ray diffraction

CRediT authorship contribution statement

Giulia Clare: Writing – review & editing, Writing – original draft, Investigation, Conceptualization. **Pedro N. Simões:** Writing – review & editing, Supervision, Resources, Funding acquisition, Conceptualization. **Irina Smirnova:** Writing – review & editing, Supervision, Resources, Funding acquisition, Conceptualization. **Luísa Durães:** Writing – review & editing, Supervision, Resources, Funding acquisition, Conceptualization.

Declaration of Generative AI and AI-assisted technologies in the writing process

The authors used ChatGPT (OpenAI) exclusively for language editing to improve the clarity and readability of the manuscript. No generative AI tools were used for data analysis, interpretation, or drafting of scientific content. The authors remain fully responsible for all content and conclusions presented.

Acknowledgements and funding

Giulia Clare acknowledges the PhD fellowship 2024.04077.BD (2024-2028), granted by Fundação para a Ciência e a Tecnologia, I.P. (FCT, Portugal), funded by national funds and co-funded by the Demography, Skills and Inclusion Thematic Program (People 2030) and Portugal 2030.

The work developed at CERES is funded by Portuguese national funds through the Fundação para a Ciência e a Tecnologia, I.P. (FCT, Portugal), in the scope of the projects doi.org/10.54499/UID/00102/2025 and doi.org/10.54499/UID/PRR/00102/2025.

Declaration of competing interest

The authors declare that they have no known competing financial interests or personal relationships that could have appeared to influence the work reported in this paper.

Data availability

No data was used for the research described in the article.

References

Abdul Khalil, H. P. S., Bashir Yahya, E., Jummaat, F., Adnan, A. S., Olaiya, N. G., Rizal, S., … Thomas, S. (2023). Biopolymers based aerogels: A review on revolutionary solutions for smart therapeutics delivery. *Progress in Materials Science, 131, Article 101014*. https://doi.org/10.1016/j.pmatsci.2022.101014

Abdullah, Zou, Y., Farooq, S., Walayat, N., Zhang, H., Faieta, M., … Huang, Q. (2022). Bio-aerogels: Fabrication, properties and food applications. *Critical Reviews in Food Science and Nutrition, 63*(24), 6687–6709. https://doi.org/10.1080/10408398.2022.2037504

Alavi, F., & Ciftci, O. N. (2024a). Green and single-step simultaneous composite starch aerogel formation-high bioavailability curcumin particle formation. *International Journal of Biological Macromolecules, 264, Article 129945*. https://doi.org/10.1016/j.ijbiomac.2024.129945

Alavi, F., & Ciftci, O. N. (2024b). Increasing the bioavailability of curcumin using a green supercritical fluid technology-assisted approach based on simultaneous starch aerogel formation-curcumin impregnation. *Food Chemistry, 455, Article 139468*. https://doi.org/10.1016/j.foodchem.2024.139468

Araujo, E. J. S., Braga, A. J. O., Monteiro Filho, J. C. K., Ndiaye, P. M., Rodrigues, R. A. F., & Martínez, J. (2024). Supercritical fluid impregnation of phenolic compounds from passion fruit bagasse in corn starch aerogels: Phase behavior and effect of operation mode. *The Journal of Supercritical Fluids, 214, Article 106387*. https://doi.org/10.1016/j.supflu.2024.106387

Araujo, E. J. S., Scopel, E., Rezende, C. A., & Martínez, J. (2023). Supercritical impregnation of polyphenols from passion fruit residue in corn starch aerogels: Effect of operational parameters. *Journal of Food Engineering, 343*, Article 111394. https://doi.org/10.1016/j.jfoodeng.2022.111394

Baudron, V., Gurikov, P., Smirnova, I., & Whitehouse, S. (2019). Porous starch materials via supercritical- and freeze-drying. *Gels, 5(1), Article 12*. https://doi.org/10.3390/gels5010012

Baudron, V., Taboada, M., Gurikov, P., Smirnova, I., & Whitehouse, S. (2020). Production of starch aerogel in form of monoliths and microparticles. *Colloid and Polymer Science, 298*(4–5), 477–494. https://doi.org/10.1007/s00396-020-04616-5

Boldrini, D. E. (2023). Starch-based materials for drug delivery in the gastrointestinal tract-A review. *Carbohydrate Polymers, 320, Article 121258*. https://doi.org/10.1016/j.carbpol.2023.121258

Braun, E., Gilmer, J., Mayes, H. B., Mobley, D. L., Monroe, J. I., Prasad, S., & Zuckerman, D. M. (2019). Best practices for foundations in molecular simulations [article v1.0]. *Living journal of computational molecular science*, *1*(1), article 5957. Doi:10.33011/livecoms.1.1.5957.

Brodkorb, A., Egger, L., Alminger, M., Alvito, P., Assunção, R., Ballance, S., Bohn, T., Bourlieu-Lacanal, C., Boutrou, R., Carrière, F., Clemente, A., Corredig, M., Dupont, D., Dufour, C., Edwards, C., Golding, M., Karakaya, S., Kirkhus, B., Le Feunteun, S., & Recio, I. (2019). INFOGEST static in vitro simulation of gastrointestinal food digestion. *Nature Protocols, 14*, 991–1014. https://doi.org/10.1038/s41596-018-0119-1

Cao, Y., Romero, J., Olson, J. P., Degroote, M., Johnson, P. D., Kieferová, M., … Aspuru-Guzik, A. (2019). Quantum chemistry in the age of quantum computing. *Chemical Reviews, 119*(19), 10856–10915. https://doi.org/10.1021/acs.chemrev.8b00803

Carpio, L. E., Sanz, Y., Gozalbes, R., & Barigye, S. J. (2021). Computational strategies for the discovery of biological functions of health foods, nutraceuticals and cosmeceuticals: A review. *Molecular Diversity, 25*, 1425–1438. https://doi.org/10.1007/s11030-021-10277-5

Chen, J., Gao, Q., Huang, M., & Yu, K. (2025). Application of modern artificial intelligence techniques in the development of organic molecular force fields. *Physical Chemistry Chemical Physics, 27*, 2294–2319. https://doi.org/10.1039/D4CP02989E

Chen, N., Chen, L., Gao, H. X., & Zeng, W. C. (2020). Mechanism of bridging and interfering effects of tea polyphenols on starch molecules. *Journal of Food Processing and Preservation, 44, Article e14576*. https://doi.org/10.1111/jfpp.14576

Chen, Z., Huang, J., Pu, H., Yang, Q., Fang, C., & Shu, G. (2020). Analysis of the complexation process between starch molecules and trilinolenin. *International Journal of Biological Macromolecules, 165*, 44–49. https://doi.org/10.1016/j.ijbiomac.2020.09.139

Cheng, L., Feng, T., Zhang, B., Zhu, X., Hamaker, B., Zhang, H., & Campanella, O. (2018). A molecular dynamics simulation study on the conformational stability of amylose-linoleic acid complex in water. *Carbohydrate Polymers, 196*, 56–65. https://doi.org/10.1016/j.carbpol.2018.04.102

Chi, C., Li, X., Feng, T., Zeng, X., Chen, L., & Li, L. (2018). Improvement in nutritional attributes of Rice starch with dodecyl Gallate complexation: A molecular dynamic simulation and in vitro study. *Journal of Agricultural and Food Chemistry, 66*(35), 9282–9290. https://doi.org/10.1021/acs.jafc.8b02121

Chopra, A. S., Lordan, R., Horbańczuk, O. K., Atanasov, A. G., Chopra, I., Horbańczuk, J. O., … Arkells, N. (2022). The current use and evolving landscape of nutraceuticals. *Pharmacological Research, 175, Article 106001*. https://doi.org/10.1016/j.phrs.2021.106001

Clare, G., Simões, P., Costa, B. F. O., & Durães, L. (2024). Dual-function starch aerogels: Nutraceutical carriers for iron and folic acid delivery. *Journal of Drug Delivery Science and Technology, 100, Article 106069*. https://doi.org/10.1016/j.jddst.2024.106069

Clare, G., Simões, P. N., & Durães, L. (2025). Encapsulation of water-soluble bioactive ingredients in starch aerogels for nutraceutical delivery. In A. Gomez-Zavaglia (Ed.),

Basic protocols in encapsulation of food ingredients. Methods and protocols in food science (pp. 69–75). Springer. https://doi.org/10.1007/978-1-0716-4148-4_8.
De Marco, I., & Reverchon, E. (2017). Starch aerogel loaded with poorly water-soluble vitamins through supercritical CO 2 adsorption. *Chemical Engineering Research and Design, 119*, 221–230. https://doi.org/10.1016/j.cherd.2017.01.024
De Marco, I., Riemma, S., & Iannone, R. (2019). Life cycle assessment of supercritical impregnation: Starch aerogel+α-tocopherol tablets. *The Journal of Supercritical Fluids, 143*, 305–312. https://doi.org/10.1016/j.supflu.2018.09.003
Dhua, S., Gupta, A. K., & Mishra, P. (2022). Aerogel: Functional emerging material for potential application in food: A review. *Food and Bioprocess Technology, 15*, 2396–2421. https://doi.org/10.1007/s11947-022-02829-w
Dias, A. L. B., Hatami, T., Viganó, J., Santos de Araújo, E. J., Mei, L. H. I., Rezende, C. A., & Martínez, J. (2022). Role of supercritical CO2 impregnation variables on β-carotene loading into corn starch aerogel particles. *Journal of CO2 Utilization, 63, Article 102125*. https://doi.org/10.1016/j.jcou.2022.102125
Druel, L., Bardl, R., Vorwerg, W., & Budtova, T. (2017). Starch aerogels: A member of the family of thermal Superinsulating materials. *Biomacromolecules, 18*(12), 4232–4239. https://doi.org/10.1021/acs.biomac.7b01272
EDQM. (2023). Harmonisation status for Excipient monographs (PDG). Retrieved April 4, 2025, from https://www.edqm.eu/en/harmonisation-status-for-excipient-monographs-pdg.
EFSA. (2019). Dietary Reference Values for the EU - DRV Finder. Retrieved April 4, 2025, from https://multimedia.efsa.europa.eu/drvs/index.htm.
EFSA. (2022). Food supplements. Retrieved April 4, 2025, from https://www.efsa.europa.eu/en/topics/topic/food- supplements.
Eliasson, A. C. (2010). Gelatinization and retrogradation of starch in foods and its implications for food quality. In L. H. Skibsted, J. Risbo, & M. L. Andersen (Eds.), *Chemical deterioration and physical instability of food and beverages (pp. 296–323)*. Elsevier. https://doi.org/10.1533/9781845699260.2.296.
EPCEU. (2002). Directive 2002/46/EC - European Parliament and Council of European Union - the approximation of the laws of the member states relating to food supplements. *Official Journal of the European Communities*, L 183/51–L 183/57. Retrieved April 4, 2025, from https://eur-lex.europa.eu/legal-content/EN/TXT/PDF/?uri=CELEX:32002L0046.
EPCEU. (2015). Regulation 2015/2283 - European Parliament and Council of European Union - novel foods. *Official Journal of the European Union*, L 327/1–L 327/22. Retrieved April 4, 2025, from https://eur-lex.europa.eu/legal-content/EN/TXT/PDF/?uri=CELEX:32015R2283.
Feng, T., Hu, Z., Wang, K., Zhu, X., Chen, D., Zhuang, H., Yao, L., Song, S., Wang, H., & Sun, M. (2020). Emulsion-based delivery systems for curcumin: Encapsulation and interaction mechanism between debranched starch and curcumin. *International Journal of Biological Macromolecules, 161*, 746–754. https://doi.org/10.1016/j.ijbiomac.2020.06.088
Feng, T., Li, M., Zhou, J., Zhuang, H., Chen, F., Ye, R., … Fang, Z. (2015). Application of molecular dynamics simulation in food carbohydrate research—A review. *Innovative Food Science & Emerging Technologies, 31*, 1–13. https://doi.org/10.1016/j.ifset.2015.06.015
Feng, T., Zhu, X., & Campanella, O. (2016). Molecular modeling tools to characterize the structure and complexation behavior of carbohydrates. *Current Opinion in Food Science, 9*, 62–69. https://doi.org/10.1016/j.cofs.2016.08.003
Ganesan, K., Budtova, T., Ratke, L., Gurikov, P., Baudron, V., Preibisch, I., … Milow, B. (2018). Review on the production of polysaccharide aerogel particles. *Materials, 11* (11), Article 2144. https://doi.org/10.3390/ma11112144
Garcia, M. A. V. T., Garcia, C. F., & Faraco, A. A. G. (2020). Pharmaceutical and biomedical applications of native and modified starch: A review. Starch - Stärke, 72 (7–8), article 1900270. doi:https://doi.org/10.1002/star.201900270.
García-González, C. A., Budtova, T., Durães, L., Erkey, C., Del Gaudio, P., Gurikov, P., Koebel, M., Liebner, F., Neagu, M., & Smirnova, I. (2019). An opinion paper on aerogels for biomedical and environmental applications. Molecules, 24(9), article 1815. doi:https://doi.org/10.3390/molecules24091815.
García-González, C. A., Jin, M., Gerth, J., Alvarez-Lorenzo, C., & Smirnova, I. (2015). Polysaccharide-based aerogel microspheres for oral drug delivery. *Carbohydrate Polymers, 117*, 797–806. https://doi.org/10.1016/j.carbpol.2014.10.045
García-González, C. A., Sosnik, A., Kalmár, J., De Marco, I., Erkey, C., Concheiro, A., & Alvarez-Lorenzo, C. (2021). Aerogels in drug delivery: From design to application. *Journal of Controlled Release, 332*, 40–63. https://doi.org/10.1016/j.jconrel.2021.02.012
Gibowsky, L., De Berardinis, L., Plazzotta, S., Manke, E., Jung, I., Méndez, D. A., … Schroeter, B. (2025). Conversion of natural tissues and food waste into aerogels and their application in oleogelation. *Green Chemistry, 27*(17), 4713–4731. https://doi.org/10.1039/D4GC05703A
Gonçalves, R. F. S., Martins, J. T., Duarte, C. M. M., Vicente, A. A., & Pinheiro, A. C. (2018). Advances in nutraceutical delivery systems: From formulation design for bioavailability enhancement to efficacy and safety evaluation. *Trends in Food Science and Technology, 78*, 270–291. https://doi.org/10.1016/j.tifs.2018.06.011
Goodfellow, B. J., & Wilson, R. H. (1990). A Fourier transform IR study of the gelation of amylose and amylopectin. *Biopolymers, 30*(13–14), 1183–1189. https://doi.org/10.1002/bip.360301304
Griffin, J. S., Bertino, M. F., Selden, T. M., Członka, S. M., & Steiner, S. A. (2023). Freeze Drying. In M. A. Aegerter, N. Leventis, M. Koebel, & S. A. Steiner, III (Eds.), *Springer Handbook of Aerogels* (pp. 121–131). Cham: Springer Handbooks. Springer. https://doi.org/10.1007/978-3-030-27322-4_5.
Hao, Z., Han, S., Zhao, Z., Wu, Z., Xu, H., Li, C., Zheng, M., Zhou, Y., Du, Y., & Yu, Z. (2024). Investigation of physicochemical properties and structure of ball milling pretreated modified starch-ferulic acid complexes. *Food Chemistry, X, 24, Article 101919*. https://doi.org/10.1016/j.fochx.2024.101919
Hao, Z., Hu, A., Cheng, J., Ma, Z., Li, Z., Lv, J., Xu, H., Ge, H., Wang, H., Yu, Z., Xie, Z., & Du, Y. (2024). Mechanism of interaction between L-theanine and maize starch in ultrasonic field based on DFT calculations: Rheological properties, multi-scale structure and in vitro digestibility. *International Journal of Biological Macromolecules, 261, Article 129869*. https://doi.org/10.1016/j.ijbiomac.2024.129869
Hao, Z., Xu, H., Yu, Y., Gu, Z., Wang, Y., Li, C., Xiao, Y., Liu, Y., Liu, K., Zheng, M., Du, Y., Zhou, Y., & Yu, Z. (2024). Insights into ball milling treatment promotes the formation of starch-lipid complexes and the relation between multi-scale structure and in vitro digestibility based on intermolecular interactions. *Food Hydrocolloids, 146, Article 109277*. https://doi.org/10.1016/j.foodhyd.2023.109277
Hatami, T., Santos, J., de Araújo, E., Dias, L. B., & A., Helena Innocentini Mei, L., & Martínez, J.. (2024). Mechanism of multicyclic β-carotene impregnation into corn starch aerogels via supercritical CO2 with mathematical modeling. *Food Research International, 178, Article 114002*. https://doi.org/10.1016/j.foodres.2024.114002
Hoover, R. (1995). Starch retrogradation. *Food Reviews International, 11*(2), 331–346. https://doi.org/10.1080/87559129509541044
Jensen, F. (2017). *Introduction to computational chemistry (3rd edition)*. John Wiley & Sons.
Jiali, L., Wu, Z., Liu, L., Yang, J., Wang, L., Li, Z., & Liu, L. (2024). The research advance of resistant starch: Structural characteristics, modification method, immunomodulatory function, and its delivery systems application. *Critical Reviews in Food Science and Nutrition, 64*(29), 10885–10902. https://doi.org/10.1080/10408398.2023.2230287
Karim, A. A., Norziah, M. H., & Seow, C. C. (2000). Methods for the study of starch retrogradation. *Food Chemistry, 71*(1), 9–36. https://doi.org/10.1016/S0308-8146(00)00130-8
Karma, V., Gupta, A. D., Yadav, D. K., Singh, A. A., Verma, M., & Singh, H. (2022). Recent developments in starch modification by organic acids: A review. *Starch - Stärke, 74*(9–10). https://doi.org/10.1002/star.202200025
Katz, J. R. (1934). The physical chemistry of starch and bread baking XX. *Journal of Physical Chemistry*, *A169*, 321.
Keith, J. A., Vassilev-Galindo, V., Cheng, B., Chmiela, S., Gastegger, M., Müller, K., & Tkatchenko, A. (2021). Combining machine learning and computational chemistry for predictive insights into chemical systems. *Chemical Reviews, 121*(16), 9816–9872. https://doi.org/10.1021/acs.chemrev.1c00107
Kistler, S. S. (1931). Coherent expanded aerogels and jellies. *Nature, 127*(3211), 741. https://doi.org/10.1038/127741a0
Labelle, M., Ispas-Szabo, P., & Mateescu, M. A. (2020). Structure-functions relationship of modified starches for pharmaceutical and biomedical applications. *Starch - Stärke, 72(7–8), Article 2000002*. https://doi.org/10.1002/star.202000002
Li, H., Lv, H.-N., Yang, T.-X., Zhao, Q.-S., & Zhao, B. (2024). Wheat starch-based aerogel for cannabidiol encapsulation: Structural analysis and enhanced stability. *Journal of Molecular Liquids, 413, Article 125923*. https://doi.org/10.1016/j.molliq.2024.125923
Li, X., Dai, L., Zhong, J., Li, T., Fan, G., Zhou, D., & Wu, C. (2024). Complexation process and binding parameters of curcumin and short amylose with V7-type helix structure. *Grain & Oil Science and Technology, 7*(4), 246–253. https://doi.org/10.1016/j.gaost.2024.09.001
Li, X., Li, C., Feng, J., Li, T., Zhou, D., Wu, C., & Fan, G. (2024). Insights into formation and stability mechanism of V7-type short amylose-resveratrol complex using molecular dynamics simulation and molecular docking. *International Journal of Biological Macromolecules, 265, Article 130930*. https://doi.org/10.1016/j.ijbiomac.2024.130930
Lukic, I., Pajnik, J., Tadic, V., & Milovanovic, S. (2022). Supercritical CO2-assisted processes for development of added-value materials: Optimization of starch aerogels preparation and hemp seed extracts impregnation. *Journal of CO2 Utilization, 61, Article 102036*. https://doi.org/10.1016/j.jcou.2022.102036
Maleki, H., Durães, L., García-González, C. A., del Gaudio, P., Portugal, A., & Mahmoudi, M. (2016). Synthesis and biomedical applications of aerogels: Possibilities and challenges. *Advances in Colloid and Interface Science, 236*, 1–27. https://doi.org/10.1016/j.cis.2016.05.011
Manocha, S., Dhiman, S., Grewal, A. S., & Guarve, K. (2022). Nanotechnology: An approach to overcome bioavailability challenges of nutraceuticals. *Journal of Drug Delivery Science and Technology, 72, Article 103418*. https://doi.org/10.1016/j.jddst.2022.103418
Manzocco, L., Mikkonen, K. S., & García-González, C. A. (2021). Aerogels as porous structures for food applications: Smart ingredients and novel packaging materials. *Food. Structure, 28, Article 100188*. https://doi.org/10.1016/j.foostr.2021.100188
Mehdi, S., Smith, Z., Herron, L., Zou, Z., & Tiwary, P. (2024). Enhanced sampling with machine learning. *Annual Review of Physical Chemistry, 75*, 347–370. https://doi.org/10.1146/annurev-physchem-083122-125941
Milovanovic, S., Jankovic-Castvan, I., Ivanovic, J., & Zizovic, I. (2015). Effect of starch xero- and aerogels preparation on the supercritical CO2 impregnation of thymol. Starch - Stärke, 67(1–2), 174–182. doi:https://doi.org/10.1002/star.201400134.
Mottola, S., Iannone, G., Giordano, M., González-Garcinuño, Á., Jiménez, A., Tabernero, A., Martín del Valle, E., & De Marco, I. (2023). Supercritical impregnation of starch aerogels with quercetin: Fungistatic effect and release modelling with a compartmental model. *International Journal of Biological Macromolecules, 253, Article 127406*. https://doi.org/10.1016/j.ijbiomac.2023.127406
Ollitrault, P. J., Miessen, A., & Tavernelli, I. (2021). Molecular quantum dynamics: A quantum computing perspective. *Accounts of Chemical Research, 54*(23), 4229–4238. https://doi.org/10.1021/acs.accounts.1c00514
Pantić, M., Nowak, M., Lavrič, G., Knez, Ž., Novak, Z., & Zizovic, I. (2024). Enhancing the properties and morphology of starch aerogels with nanocellulose. *Food Hydrocolloids, 156, Article 110345*. https://doi.org/10.1016/j.foodhyd.2024.110345

Patel, S., Jayakumar, P., Yen, T., & Izmaylov, A. F. (2025). Quantum measurement for quantum chemistry on a quantum computer. *Chemical Reviews, 125*(16), 7490–7524. https://doi.org/10.1021/acs.chemrev.5c00055

Patil, S. P., Parale, V. G., Park, H.-H., & Markert, B. (2021). Mechanical modeling and simulation of aerogels: A review. *Ceramics International, 47*(3), 2981–2998. https://doi.org/10.1016/j.ceramint.2020.09.181

Poma, A. B., Caldas, A. H., Cofas-Vargas, L. F., Jones, M. S., Ferguson, A. L., & Sandonas, L. M. (2025). Recent advances in machine learning and coarse-grained potentials for biomolecular simulations. *Biophysical Journal. Advance online publication.*. https://doi.org/10.1016/j.bpj.2025.06.019

Puri, V., Nagpal, M., Singh, I., Singh, M., Dhingra, G. A., Huanbutta, K., … Sangnim, T. (2022). A comprehensive review on nutraceuticals: Therapy support and formulation challenges. *Nutrients, 14(21), Article 4637*. https://doi.org/10.3390/nu14214637

Rostamabadi, H., Falsafi, S. R., & Jafari, S. M. (2019). Starch-based nanocarriers as cutting-edge natural cargos for nutraceutical delivery. *Trends in Food Science & Technology, 88*, 397–415. https://doi.org/10.1016/j.tifs.2019.04.004

Sang, S., Xu, X., Zhu, X., & Narsimhan, G. (2021). Complexation of 26-Mer amylose with egg yolk lipids with different numbers of tails using a molecular dynamics simulation. *Foods, 10(10), Article 2355*. https://doi.org/10.3390/foods10102355

Schroeter, B., Jeansathawong, P., Hajnal, A., & Gurikov, P. (2023). Wet milling of alginate Alco- and hydrogel composites: A facile top-down approach for continuous production of aerogel microparticles. *Macromolecular Materials and Engineering, 308*, Article 2200674. https://doi.org/10.1002/mame.202200674

Selmer, I., Behnecke, A., Quiño, J., Braeuer, A. S., Gurikov, P., & Smirnova, I. (2018). Model development for sc-drying kinetics of aerogels: Part 1. Monoliths and single particles. *The Journal of Supercritical Fluids, 140*, 415–430. https://doi.org/10.1016/j.supflu.2018.07.002

Selvasekaran, P., & Chidambaram, R. (2021). Food-grade aerogels obtained from polysaccharides, proteins, and seed mucilages: Role as a carrier matrix of functional food ingredients. *Trends in Food Science & Technology, 112*, 455–470. https://doi.org/10.1016/j.tifs.2021.04.021

Selvasekaran, P., & Chidambaram, R. (2022). Bioaerogels as food materials: A state-of-the-art on production and application in micronutrient fortification and active packaging of foods. *Food Hydrocolloids, 131, Article 107760*. https://doi.org/10.1016/j.foodhyd.2022.107760

Shao, M., Li, S., Tan, C. P., Kraithong, S., Gao, Q., Fu, X., … Huang, Q. (2021). Encapsulation of caffeine into starch matrices: Bitterness evaluation and suppression mechanism. *International Journal of Biological Macromolecules, 173*, 118–127. https://doi.org/10.1016/j.ijbiomac.2021.01.043

Siddiqui, R. A., & Moghadasian, M. H. (2020). Nutraceuticals and nutrition supplements: Challenges and opportunities. Nutrients, 12(6), article 1593. doi:https://doi.org/10.3390/nu12061593.

Soleimanpour, M., Tamaddon, A. M., Kadivar, M., Abolmaali, S. S., & Shekarchizadeh, H. (2020). Fabrication of nanostructured mesoporous starch encapsulating soy-derived phytoestrogen (genistein) by well-tuned solvent exchange method. *International Journal of Biological Macromolecules, 159*, 1031–1047. https://doi.org/10.1016/j.ijbiomac.2020.05.124

Span, R., & Wagner, W. (1996). A new equation of state for carbon dioxide covering the fluid region from the triple-point temperature to 1100 K at pressures up to 800 MPa. *Journal of Physical and Chemical Reference Data, 25*(6), 1509–1596. https://doi.org/10.1063/1.555991

Steiner, S. A., & Pierre, A. C. (2023). The story of aerogel. In M. A. Aegerter, N. Leventis, M. Koebel, & S. A. Steiner, III (Eds.), *Springer Handbook of Aerogels* (pp. 1–50). Cham: Springer. https://doi.org/10.1007/978-3-030-27322-4_1.

Subrahmanyam, R., Selmer, I., Bueno, A., Weinrich, D., Lölsberg, W., Fricke, M., … Smirnova, I. (2023). Supercritical drying of aerogels. In M. A. Aegerter, N. Leventis, M. Koebel, & S. A. Steiner, III (Eds.), *Springer Handbook of Aerogels* (pp. 93–120). Cham: Springer. https://doi.org/10.1007/978-3-030-27322-4_4.

Sun, C., Wei, Z., Xue, C., & Yang, L. (2023). Development, application and future trends of starch-based delivery systems for nutraceuticals: A review. *Carbohydrate Polymers, 308, Article 120675*. https://doi.org/10.1016/j.carbpol.2023.120675

Tian, S., Xue, X., Wang, X., & Chen, Z. (2022). Preparation of starch-based functional food nano-microcapsule delivery system and its controlled release characteristics. *Frontiers in Nutrition, 9*, 1–14. https://doi.org/10.3389/fnut.2022.982370

Ubeyitogullari, A., & Ciftci, O. N. (2016). Phytosterol nanoparticles with reduced crystallinity generated using nanoporous starch aerogels. *RSC Advances, 6*(110), 108319–108327. https://doi.org/10.1039/C6RA20675A

Ubeyitogullari, A., Moreau, R., Rose, D. J., Zhang, J., & Ciftci, O. N. (2019). Enhancing the bioaccessibility of Phytosterols using Nanoporous corn and wheat starch bioaerogels. *European Journal of Lipid Science and Technology, 121*(1), Article 1700229. https://doi.org/10.1002/ejlt.201700229

Unke, O. T., Chmiela, S., Sauceda, H. E., Gastegger, M., Poltavsky, I., Schütt, K. T., … Müller, K. (2021). Machine learning force fields. *Chemical Reviews, 121*(16), 10142–10186. https://doi.org/10.1021/acs.chemrev.0c01111

US FDA. (2024). 21 CFR 184.1240 Carbon dioxide, in Code of Federal Regulations. Retrieved July 9, 2025, from https://www.ecfr.gov/current/title-21/part-184/section-184.1240.

Vareda, J. P., Lamy-Mendes, A., & Durães, L. (2018). A reconsideration on the definition of the term aerogel based on current drying trends. *Microporous and Mesoporous Materials, 258*, 211–216. https://doi.org/10.1016/j.micromeso.2017.09.016

Villegas, M., Oliveira, A. L., Bazito, R. C., & Vidinha, P. (2019). Development of an integrated one-pot process for the production and impregnation of starch aerogels in supercritical carbon dioxide. *The Journal of Supercritical Fluids, 154, Article 104592*. https://doi.org/10.1016/j.supflu.2019.104592

Wang, S., Li, C., Copeland, L., Niu, Q., & Wang, S. (2015). Starch Retrogradation: A comprehensive review. *Comprehensive Reviews in Food Science and Food Safety, 14*(5), 568–585. https://doi.org/10.1111/1541-4337.12143

Wang, Y., Liu, T., Xie, J., Cheng, M., Sun, L., Zhang, S., Xin, J., & Zhang, N. (2022). A review on application of molecular simulation technology in food molecules interaction. *Current Research in Food Science, 5*, 1873–1881. https://doi.org/10.1016/j.crfs.2022.10.012

Wang, Z., Li, Y., Chen, L., Xin, X., & Yuan, Q. (2013). A study of controlled uptake and release of anthocyanins by oxidized starch microgels. *Journal of Agricultural and Food Chemistry, 61*(24), 5880–5887. https://doi.org/10.1021/jf400275m

WebBook, N. I. S. T. (2025). Carbon dioxide. Retrieved July 31, 2025, from https://webbook.nist.gov/cgi/cbook.cgi?Mask=4&Source=1978JON%2FTAY1768&Units=SI.

Wildman, R. E. C. (2007). *Handbook of nutraceuticals and functional foods second edition (2nd edition)*. CRC Press.

Witkowski, A., Majkut, M., & Rulik, S. (2014). Analysis of pipeline transportation systems for carbon dioxide sequestration. *Archives of Thermodynamics, 35*(1), 117–140. https://doi.org/10.2478/aoter-2014-0008

Wu, Y., He, D., Zong, M., Wu, H., Li, L., Zhang, X., … Li, B. (2022). Improvement in the stability and bioavailability of trans-resveratrol with hydrolyzed wheat starch complexation: A theoretical and experimental study. *Food. Structure, 32, Article 100267*. https://doi.org/10.1016/j.foostr.2022.100267

Xie, L., Zhang, Y., Chen, L., Wang, T., Zhang, S., & Li, X. (2024). Structural changes of layer-by-layer self-assembled starch-based nanocapsules in the gastrointestinal tract: Implications for their M cell-targeting delivery and transport efficiency. *International Journal of Biological Macromolecules, 261, Article 129786*. https://doi.org/10.1016/j.ijbiomac.2024.129786

Yang, T.-X., Li, H., Zhu, Y., Gao, Y., Lv, H.-N., Zha, S.-H., Sun, X.-L., & Zhao, Q.-S. (2024). Preparation and characterisation of wheat starch-based aerogels for procyanidin encapsulation to enhance stability. *New Journal of Chemistry, 48*(1), 79–88. https://doi.org/10.1039/D3NJ03311B

Zhang, J., Li, F., Shen, S., Yang, Z., Ji, X., Wang, X., Liao, X., & Zhang, Y. (2023). More simple, efficient and accurate food research promoted by intermolecular interaction approaches: A review. *Food Chemistry, 416, Article 135726*. https://doi.org/10.1016/j.foodchem.2023.135726

Zhang, P., Wang, Y., Liu, Y., Wu, Y., & Ouyang, J. (2023). Improved stability of β-carotene by encapsulation in SHMP-corn starch aerogels. *Food Chemistry, 406, Article 135040*. https://doi.org/10.1016/j.foodchem.2022.135040

Zhang, Z., Feng, Y., Wang, H., & He, H. (2024). Synergistic modification of hot-melt extrusion and nobiletin on the multi-scale structures, interactions, thermal properties, and in vitro digestibility of rice starch. *Frontiers. Nutrition, 11, Article 1398380*. https://doi.org/10.3389/fnut.2024.1398380

Zhao, S., Malfait, W. J., Guerrero-Alburquerque, N., Koebel, M. M., & Nyström, G. (2018). Biopolymer-Aerogele und -Schäume: Chemie, Eigenschaften und Anwendungen. *Angewandte Chemie, 130*(26), 7704–7733. https://doi.org/10.1002/ange.201709014

Zheng, Q., Tian, Y., Ye, F., Zhou, Y., & Zhao, G. (2020). Fabrication and application of starch-based aerogel: Technical strategies. *Trends in Food Science and Technology, 99*, 608–620. https://doi.org/10.1016/j.tifs.2020.03.038

Zhou, H., Tan, Y., & McClements, D. J. (2023). Applications of the INFOGEST in vitro digestion model to foods: A review. *Annual Review of Food Science and Technology, 14*, 135–156. https://doi.org/10.1146/annurev-food-060721-012235

Zhu, F. (2019). Starch based aerogels: Production, properties and applications. *Trends in Food Science & Technology, 89*, 1–10. https://doi.org/10.1016/j.tifs.2019.05.001

Zhu, Y., Li, H., Peng, C., Ma, J., Huang, S., Wang, R., Wu, B., Xiong, Q., Peng, D., Huang, S., & Chen, J. (2023). Application of protein/polysaccharide aerogels in drug delivery system: A review. *International Journal of Biological Macromolecules, 247*, Article 125727. https://doi.org/10.1016/j.ijbiomac.2023.125727

Zou, F., & Budtova, T. (2021). Tailoring the morphology and properties of starch aerogels and cryogels via starch source and process parameter. *Carbohydrate Polymers, 255*, Article 117344. https://doi.org/10.1016/j.carbpol.2020.117344

Zou, F., & Budtova, T. (2023). Starch Alcogels, aerogels, and aerogel-like Xerogels: Adsorption and release of theophylline. *ACS Sustainable Chemistry & Engineering, 11*(14), 5617–5625. https://doi.org/10.1021/acssuschemeng.2c07762